UNIVERSITÀ DI PARMA

UNIVERSITÀ DEGLI STUDI DI PARMA

Ph.D. Course in
"Drugs, Biomolecules and Health Products"

XXXI Cycle

EXPERIMENTAL STRATEGY FOR THE IDENTIFICATION AND CHARACTERIZATION OF NOVEL INHIBITORS OF ALKYLQUINOLONE-DEPENDENT QUORUM SENSING REGULATOR IN *PSEUDOMONAS AERUGINOSA*, A PROMISING ANTIBACTERIAL TARGET

Coordinator:
Prof. Dr. Marco Mor
Supervisor:
Prof. Dr. Andrea Mozzarelli
Advisor:
Dr. Antonio Felici

PhD student: Vanesa Garrido Estevez

Year **2015/2018**

EXPERIMENTAL STRATEGY FOR THE IDENTIFICATION AND CHARACTERIZATION OF NOVEL INHIBITORS OF ALKYLQUINOLONE-DEPENDENT QUORUM SENSING REGULATOR IN PSEUDOMONAS AERUGINOSA, A PROMISING ANTIBACTERIAL TARGET

Vanesa Garrido Estevez

The studies described in this thesis were performed at the Department of Microbiology, Aptuit, and Evotec Company (Italy) and at University of Parma (Italy).
This project has received funding from the European Union's Horizon 2020 research and innovation programme under the Marie Sklodowska Curie grant agreement No 642620.

CONTENTS

Chapter 1

General Introduction

ANTIMICROBIAL RESISTANCE

Drug resistant bacteria are a global public health threat that is getting worse [1]. An estimated 700,000 people die each year around the world from drug-resistant bacteria, according to the World Health Organization (WHO). In the US alone, the Centers for Disease Control and Prevention (CDC) estimates that 23,000 people die each year, and the European Centre for Disease Prevention and Control (ECDC) estimates that 25,000 people die annually in Europe [2].

Many advances of modern medicine — joint replacements, organ transplants, cancer therapy, and treatment of chronic diseases such as diabetes, asthma or cystic fibrosis — are dependent on the ability to fight infections with antibiotics. If that ability is lost, also the power to safely offer people many life-saving and life-improving modern medical advantages will also be.

Part of the solution is to accelerate the development of new drugs to treat drug-resistant infection. No newly approved classes of antibiotics have been discovered since 1962 for the most dangerous types of Gram negative bacteria, and innovations to improve the diagnosis and prevention of drug-resistant infections have been slow [3].

Most large drug companies have reduced or abandoned infection research due to scientific challenges, and because it has become impossible for them to recoup the cost of research [4].

The economic model that once meant we could rely on industry for a steady supply of new antibiotics simply no longer works. At the same time, the deadliest superbugs have been rapidly developing resistance to existing antibiotics, hastened by overuse and misuse in humans and animals. It takes on average 10 years and hundreds of millions of dollars to develop a new drug [5]. Superbugs can develop resistance much faster.

In September 2017, the World Health Organization (WHO) published the outcome of a huge work on prioritization of pathogens aiming to guide discovery, research and development of new antibiotics for drug-resistant bacterial infections, including tuberculosis. In the priority list of antibiotic-resistant pathogens requiring urgent attention, *P. aeruginosa* ranked at second position because of its multidrug resistance to a broad spectrum of antibiotics including carbapenems and third generation of cephalosporin [6], [7].

One year later, in September 2018, the Pew Analyses on conventional antibacterial agents in clinical development showed a severe gap in global pipeline, which needs a big discovery need push [8]. Only half of the projects have activity against WHO priority list, only four advanced candidates have potential activity against 'most urgent' pathogens (Figure 1), few new targets, few new chemical series and few new mechanism-of-action are novel, and, finally, very few resistance breakers are present.

A recent European Antimicrobial Resistance Surveillance Network (EARS-Net) study shows that a 30.8% of *P. aeruginosa* tested isolates were resistance to at least one of the antimicrobial groups under regular surveillance [9]. In particular, the highest EU/EEA population-weighted mean resistance percentage in 2017 was reported for fluoroquinolones (20.3%), followed by piperacillin ± tazobactam (18.3%), carbapenems (17.4%), ceftazidime (14.7%) and aminoglycosides (13.2%) (Figure 2). These data suggest the new *anti-pseudomonas* drugs and treatments do not overcome the serious antimicrobial resistance problem present nowadays. Actually the pharmaceutical industry focused their research on looking for new antibiotics or improved delivery systems to achieve the target or the site of infection [10].

However these approaches only slow the rate of the emergence of multidrug resistance bacteria. With an encouraging perspective, it is necessary to

develop alternative approach to classic antimicrobial therapies such as targeting bacterial virulence [11], which offers promising opportunities by which only pathogenicity and not survival/fitness relevant traits are affected [12].

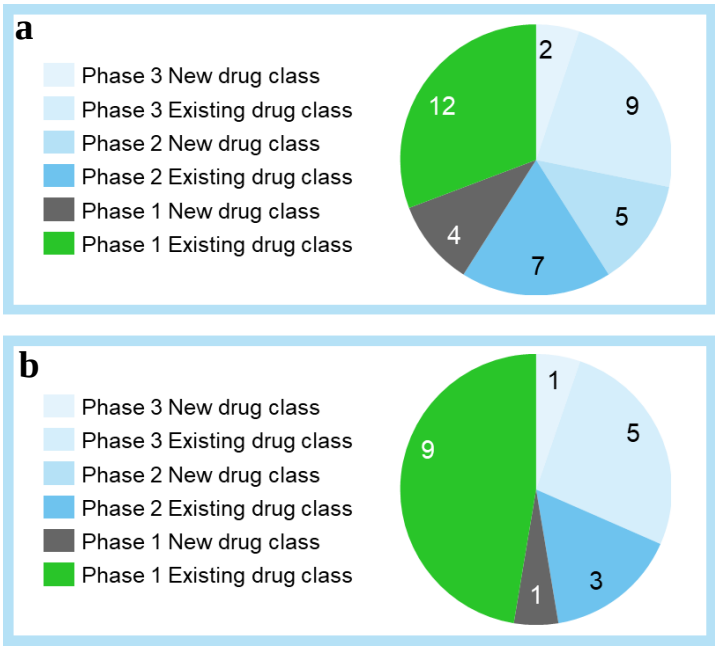

Figure 1. Antibacterial agents in clinical development against a) all bacteria b) critical list.

In this way selective resistance is limited without placing life or death pressure on the target bacterium. Among the several and various strategies put in place in the discovery of novel therapies against multi-drug (MDR) or extreme-drug resistant pathogens (EDR), targeting specific quorum sensing system [13], which regulates virulence expression in all Gram-negative pathogens, including *P. aeruginosa*, has been proposed with the objective of blocking production of auto-inducers molecules, which are necessary to regulate group behaviours playing an important role in acute and/or chronic infection process.

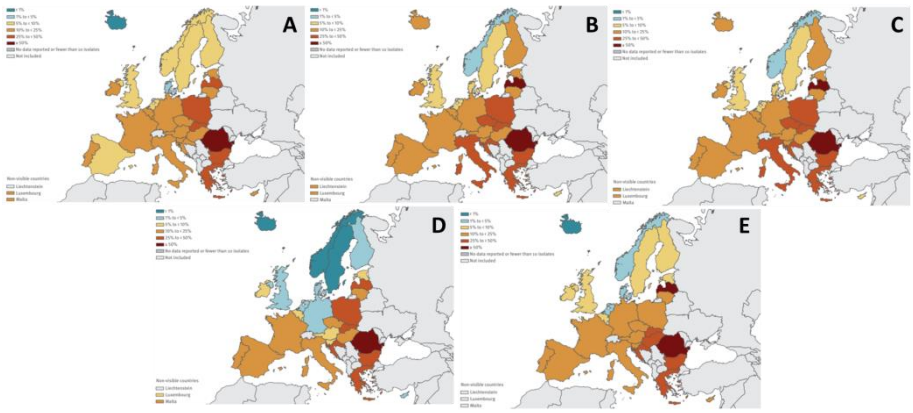

Figure 2. Percentage (%) of invasive *P. aeruginosa* isolates with resistance to A) piperacillin±tazobactam, B) fluoroquinolones, C) ceftazidime, D) aminoglycosides and E) carbapenems, by country (EU/EEA), 2017.

PSEUDOMONAS AERUGINOSA

Pseudomonas aeruginosa is an opportunistic Gram-negative pathogen that causes serious acute, persistent and relapsing infections. This Gram negative pathogen presents a wide range of resistant to many antibiotics and it shows intrinsically advanced resistance to antibiotics due not only to the low-permeability of its outer-membrane [14] but also to the presence of efflux pumps and the production of β-lactamase, antibiotic inactivating enzymes supplying resistance against penicillin and cephalosporin [15]. The efflux pumps molecular machineries, on the other hand, have the main function of expel antibiotics such as cephalosporins, carbapenems, fluoroquinolones and aminoglycosides [16]. In addition to all the above, *P. aeruginosa* is able to acquire resistance mainly by horizontal gene transfer but can also be induced by different spontaneous mutations in genes encoding for target protein or leading to efflux pump overexpression [17]. Clearly, these resistance mechanisms make *P. aeruginosa* infection difficult to eradicate. Usual sites

of infection of this ubiquitous pathogen are the urinary and respiratory tracts as well as wounds resulting from burn injuries [18]. These infections occur mainly in immunocompromised individuals such as those patients suffering from cystic fibrosis. Representative rates of colonization in healthy humans are normally 0 – 2 % for skin, 0 – 3.3% for the nasal mucosa and 0-6.6% for the throat whereas rates of colonization in compromised individuals may be over 50% [19].

P. aeruginosa is recognized as one of the principal pulmonary pathogens that colonised young CF patients and prevail during time. *P. aeruginosa* colonisation in CF airways is correlated with loss of lung function, high morbidity and mortality of patients. In fact, the major cause of death related with this genetic disorder is the chronic colonisation of *P. aeruginosa* [20].

Thus, there is an urgent need for novel approaches, including new pharmacotherapies to treat patients infected by *P. aeruginosa* as the effectiveness of molecules targeting *P. aeruginosa* infections will be threaten by mechanisms of defence mentioned above.

ROLE OF QUORUM SENSING IN *P. AERUGINOSA*

Quorum sensing (QS) is a cell-to-cell communication system used by both Gram-positive and Gram-negative bacteria to regulate gene expression in response to changes on cell population. Several systems have been characterised, such as those from *Vibrio fischeri*, *P. aeruginosa*, and *S. aureus*. Basically, quorum sensing in bacteria is based on production and release of chemical signal molecules, called auto-inducers, which increase in concentration as a function of cell density. The detection of a minimal threshold stimulatory concentration of an auto-inducer leads to an alteration in gene expression [21]. In particular, *P. aeruginosa* pathogen uses quorum sensing system to control the expression of many virulence factors and

biofilm formation; as such, this regulation is believed to play and important role in pathogenicity during infection due to this important pathogen.

P. aeruginosa presents 4 main QS systems: las, rhl, pqs and iqs [22]. Each system produces and responds to specific auto-inducers: alkyl homoserine lactones (AHLs) are used by las and rhl systems, alkyl-quinolones (AQs) are used by pqs system and 2-(2-hydroxyphenyl)-thiazole-4-carbaldehyde is used by the iqs system. All these systems are hierarchically interconnected to each other (Figure 3). Las system positively regulates rhl, pqs and iqs systems. Rhl system activates the expression of its own *rhlI*, forming a positive feedback loop. On the other hand, rhl system inhibits pqs circuit. Iqs is the subsystem discovered more recently and it appears to have a role in positively activating both rhl and pqs systems.

All these 4 quorum sensing have been studied in depth with the aim of designing quorum sensing inhibitors to be used as blockers of *P. aeruginosa* pathogenicity.

The research of inhibitors able to block las and rhl quorum sensing systems has been extendedly studied while to the date only one study on iqs inhibition has been reported. A great effort was also made for pqs inhibitors. In fact, whole-cell high-throughput screen together with a SAR analysis, ligand based design or fragment based design using SPR, are some of the strategies that have been used for the identification of pqs QS inhibitors [23], [24].

THE PQS QS SYSTEM

Pqs quorum sensing system is controlled by a specific transcription factor, the Multiple virulence Factor Regulator (MvfR) - also known as PqsR. MvfR is activated by *Pseudomonas* quinolone signal (PQS) and its precursor 2-heptyl-4-hydroxyquinoline (HHQ). Through the interaction with this receptor, PQS and HHQ induce the expression of specific genes in the *pqsABCDE* and *phnAB* operons, ultimately encoding enzymes that catalyse

the biosynthesis of at least 57 distinct low-molecular-weight compounds, as well as their own biosynthetic cascade. The conversion of HHQ to PQS is regulated by the las system through the activity of the LasR-controlled enzyme PqsH [25]. Furthermore, the products of *phnAB* gene synthesize quinolone that regulate *phzRABCDEFG* operons 1 and 2 responsible for phenazines synthesis, such as pyocyanin (5-*N*-methyl-1-hydroxyphenazine), one of the major virulence factor produced *P. aeruginosa* [26].

PQS QS SYSTEM BIOSYNTHETIC PATHWAY

The production of PQS that refers to 2-heptyl-3-hydroxyquinolin-4-(1H)-one molecule starts from anthranilic acid (AA) which is synthesized from chorismate by antranilate synthase encoded by the *phnAB* operon. Consecutively, the AA is converted into anthraniloyl-CoA by PqsA protein with acyl-CoA ligase activity [27]. Then, PqsD binds anthraniloyl-CoA and catalyses a reaction with malonyl-CoA to produce a CoA-active 2-aminobenzoylacetate (2-ABA-CoA) [28]. Subsequently, the pathway-specific thioesterase PqsE protein cleaves the thioester bond of 2-ABA-CoA in order to get the reactive intermediate 2'-aminobenzoylacetate (2-ABA) [29]. It has been shown that also the thioesterase TesB present in *P. aeruginosa* can catalysed this reaction [29]. In the next step, 2-ABA is transformed into 4-hydroxy-2-heptylquinoline (HHQ) after the condensation of octanoyl-CoA catalysed by the activity of the heterodimeric complex PqsBC [30]. At last, HHQ is released into the extracellular milieu where it is internalized via adjacent cells and then oxidized to PQS via NADH-dependent Flavin mono-oxygenase PqsH [31]. The biosynthetic cascade is also responsible for the generation of pqs-related metabolites such as DHQ, HQNO and 2-AA [30], [32].

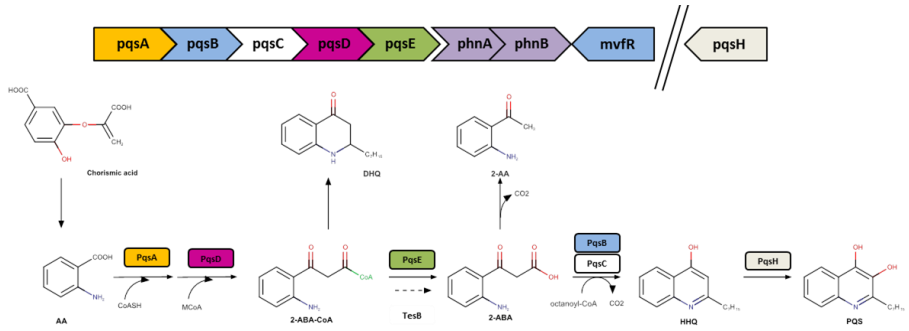

Figure 3.MvfR HAQs molecules ,2-AA and DHQ molecules biosynthetic pathway. Representation of both *pqsABCDE* and *phnAB* operon.

PATHOGENICITY TRAITS

P. aeruginosa virulence mechanisms are essential for this opportunistic pathogen to overwhelm the host in the infection process [33]. The secretion of virulence factors is mainly regulated through quorum sensing and pqs QS plays a fundamental role in the regulation of many of those.

In terms of pathogenicity, the autoinducer (AI) PQS has been demonstrated to induce membrane vesicle formation and also to act as ferric iron chelator [34], [35]. Interestingly, PQS and its precursor HHQ are able to down-regulate host innate immune system by interfering with nuclear transcription factor-κB and hypoxia-inducible factor 1 (HIF-1) [36], [37]. Furthermore, pqs QS is involved in the regulation of genes encoding for enzymes responsible of phenazines biosynthesis, persistence and biofilm formation [26]. Among the virulence factor directly correlated with pqs QS system, pyocyanin is one of the most extended. This redox toxin pigment interferes with multiple eukaryotic cells functions e.g., cell respiration, ciliary beating, epidermal cell growth apoptosis in neutrophils or delayed to inflammatory response to *P. aeruginosa* infections through neutrophil damage [38], [39]. Pyocyanin also inhibits microbial growth via a redox cascade. Consequently,

these antimicrobial properties of pyocyanin allow *P. aeruginosa* to dominate other microbes in the infection site such as in cystic fibrosis airways [40]. Other pqs-related metabolites have been shown to have additional effects, such as the small volatile 2-AA molecule, which promotes the emergence of persister *P. aeruginosa* cells formation that likely led to chronic infections [41].

Hence, targeting this regulatory system is very engaging for blocking *P. aeruginosa* pathogenicity.

MULTIVIRULENCE FACTOR REGULATOR (MvfR) AND QSI

The multivirulence transcriptional factor regulator (MvfR), also known as PqsR, is a membrane-associated protein that is mainly expressed in the late exponential phase of bacterial growth [42]. MvfR belongs to the LysR family of transcriptional regulators (LTTRs), which represents the most abundant type of transcriptional regulator in the prokaryotic kingdom. The nosocomial pathogen *P. aeruginosa* seems to have one of the largest LTTRs repertoires [43]. The LTTRs proteins possess a C- terminal ligand-binding domain, also known as co-inducer binding domain (CBD), connected via α-helix to an N-terminal helix-turn-helix (HTH) domain which is highly preserved [44]. Structural analyses have been hampered by the inability to crystallize full-length LTTR proteins due to their poor solubility. For this reason, structural studies of LTTRs have been restricted to the C-terminal ligand-binding domain. It has been shown that interfering with MvfR transcriptional regulator decreased virulence factor production, disrupts biofilm and increases the sensitivity for antibiotics [24], [32]. With respect to MvfR, many studies elucidated the structural basis for the recognition of HAQs by MvfR, [45]–[48] in order to provide molecular detail to facilitate the

development of MvfR inhibitors as novel therapeutics. Basically, the $MvfR^{CBD}$ structure has two subdomains connected by antiparallel β-sheet called the hinge region, with a hydrophobic ligand binding pocket between the two subdomains. Native ligands such as PQS and HHQ bind to same binding pocket as some potent inhibitors reporter into the literature e.g., QZN or M64 [46], [47]. In 2014, Starky *et al.* identified the benzamide-benzimidazole (BB) structure as a promising scaffold for the inhibition of MvfR [24]. Among all this chemical serie, the M64, a high hydrophobic compound, has been shown to be the most potent inhibitor in a low micromolar range. This BB inhibitor is able to reduce the production of pyocyanin as well as PQS and HHQ autoinducers levels. Further investigations, reveal that M64 also reduce 2-AA levels leading to a decrease rate of persisters cells without perturbing bacterial growth [41]. Interestingly, the M64-BB inhibitor binds, like native ligands, to the MvfR hydrophobic cavity where hydrogen bond with Gln194 and π-interaction with Tyr258 were important for its affinity [47]. Because of its hydrophobicity, M64 is not and ideal candidate to enter into clinical trials. In fact, some chemical efforts should be applied in order to improve solubility or decrease cytotoxicity due to the nitro aromatic residue. However, M64 is a really good template for the development of next generation of antivirulence compounds.

Through that structural information, employing *in silico* methods allowed proposing plausible binding poses for prototypic analogues of the benzamide-benzamidazole (BB) structural classes.

TARGETING TRANSCRIPTIONAL FACTOR MVFR

For the last decades, the potential of interference with quorum sensing by small chemical compounds has been investigated with the aim of developing alternative antibacterial strategies. Actually, the research of inhibitors in

order to block las and rhl quorum sensing systems has been extendedly studied [33], [49]. However, the potential of las and rhl targeting approaches decreases after the discovered that both systems were the first to be lost upon chronification of *P. aeruginosa* infections [50]. Unlike, it has been detected quinolone quorum sensing molecules, in the sputum obtained from CF patients [51], [52]. This data suggests that pqs QS circuit remain active in chronic CF patients. Different approaches were considered to inhibit pqs QS system. Enzymes belong to the biosynthesis cascade *pqsA-E*, for example, were evaluated and studied as drug targets. Derivates from anthranilic acid were used as PqsA inhibitors while 2-benzamidobenzoic acid as PqsD inhibitors, the second enzyme in the biosynthesis cascade. Anyway, targeting the receptor MvfR results in more pronounced pathoblocking effects than harp on block biosynthetic enzyme cascade.

Furthermore, it has been well demonstrated up to the date, that interfering with MvfR transcriptional regulator decreased virulence factor production, disrupts biofilm and increases the sensitivity for antibiotics, leading to an unambiguous antivirulence effect.

EARLY DRUG DISCOVERY PROCESS FOR MvfR QUOURM SENSING INHIBITORS

The first step of early drug discovery is the identification of a competent drug target and its validation through biological/biochemical assays and animal model experiments. In order to promote a hit and lead compound into the clinic, challenging efforts are needed. Due to the complex nature of virulence phenotype assays the experimental cascade is a big challenge on quorum sensing inhibitors discovery field. The usual timelines expected for non-anti-infectives drug are somehow a lit bit unreliable for the identification of quorum sensing inhibitors. Hence, there is an urgent need for current anti-

infectives discovery efforts. However, we believe that a specific experimental cascade for a specific target is quite promising.

Specifically in this project, we develop an integrated screening cascade for the selection and *in vitro* and *in vivo* evaluation of novel MvfR inhibitors.

In the past, MvfR-regulon of *P. aeruginosa* was identify and validate as a promising Quorum Sensing target for reduction of *P. aeruginosa* virulence during both acute and chronic infection in CF patients [24], [32].

Following the general steps of early drug discovery process, the identification of possible modulators of the target will be done. In the present study, a structure-feature-based modeling approach, based on the available X-ray structure of our target, was designed in order to identify a set of compounds that target the MvfR-regulon.

The next step is developing virulence phenotype assays to screen modulators. Based on that, the set of compounds selected from *in silico* screening were tested using a simple HTS spectrophotometric method in order to measure the inhibition of pyocyanin (final signal of MvfR-QS pathway) production in *P. aeruginosa* in the presence of MvfR-regulon inhibitors.

Primary phenotypic pyocyanin-driven HTS assay allowed us to identify two hits compounds able to inhibit this virulent factor produced by *P. aeruginosa*. Carry on with the early drug discovery process, a secondary assay for the identity of the hits and the most suitable profile to lead optimization is necessary. Thus, HAQs molecules (HHQ/PQS) quantitative LC/MS-MS assay was performed among the two hits compounds. A decision in function of this secondary screening was taken to follow up. Small medicinal chemistry modifications over the hit were performed in order to improve "*drug-like*" characteristics and inhibitory activity. Analogs of the hit were evaluated using phenotype assays and biomolecular interactions assays to well characterize them and decide whether some or all of them are suitable candidates to proceed with *in vivo* model (Figure 4).

OBJECTIVE OF THE THESIS

The main objective of the work carried out was to develop and validate a tailored screening cascade, with the support of multiple discovery functions, able to aid the selection and the characterization of potential new chemical templates able to modulate the MvfR QS system in *P. aeruginosa*, thus providing new starting points for wider exploration for future lead optimization effort.

Relevant *in vitro* assays for evaluation of inhibitory activity of the compounds on the MvfR system have been set up and evaluation of the binding affinity to the transcriptional modulator by Surface Plasmon Resonance was developed.

In collaboration with the Computational Science Group, a structure-based *in silico* screening approach based on docking studies of M64 molecule with the purpose of identifying suitable hits was carried out.

In vitro suit HTP pyocyanin screening assays, 96/-well-MTP pyocyanin, were set up to support hit confirmation and selection. *In vitro* potency, effect on HAQs molecules expression and interaction on the target was also performed.

In parallel, with the aim to select a sub-panel of *P. aeruginosa* strains representative of the population characterizing cystic fibrosis infection, to be utilized for efficacy studies in model of bacterial infections in rodent species, a wide panel of *P. aeruginosa* isolates collected from the sputum of CF patients was *in vitro* characterized in terms of pyocyanin and HAQs molecules production, biofilm formation and antimicrobial susceptibility profile.

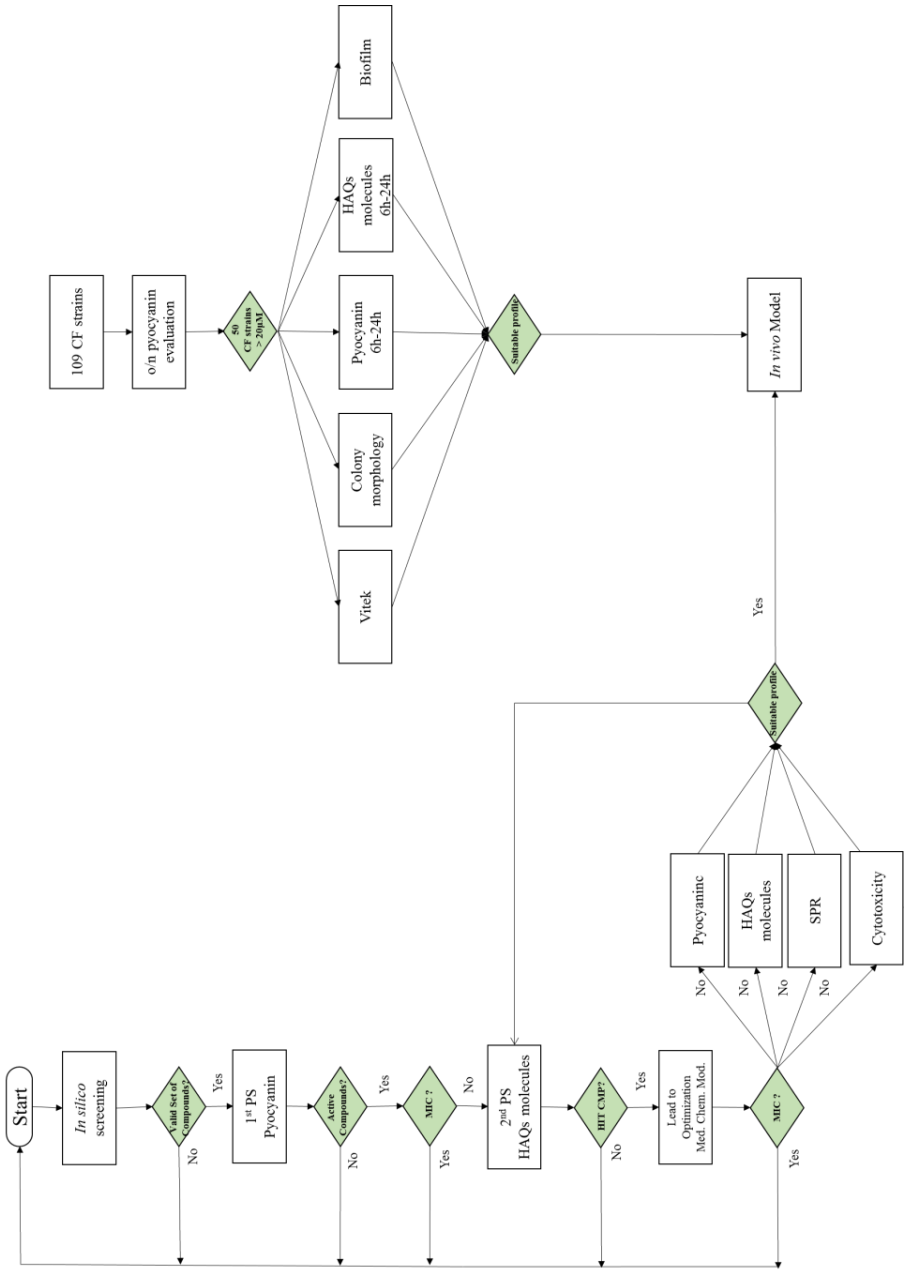

Figure 4. Project Assay Cascade for MvfR-regulon inhibitors identification and characterization.

REFERENCE

[1] H. D. Marston, D. M. Dixon, J. M. Knisely, T. N. Palmore, and A. S. Fauci, 'Antimicrobial resistance', *JAMA - J. Am. Med. Assoc.*, vol. 316, no. 11, pp. 1193–1204, 2016.

[2] European Centre for Disease Prevention and Control, *SURVEILLANCE REPORT: Antimicrobial resistance surveillance in Europe 2014*. 2014.

[3] L. J. V Piddock, 'The crisis of no new antibiotics-what is the way forward?', *The Lancet Infectious Diseases*. 2012.

[4] J. G. Bartlett, D. N. Gilbert, and B. Spellberg, 'Seven ways to preserve the Miracle of antibiotics', *Clinical Infectious Diseases*. 2013.

[5] K. H. Luepke *et al.*, 'Past, Present, and Future of Antibacterial Economics: Increasing Bacterial Resistance, Limited Antibiotic Pipeline, and Societal Implications', *Pharmacotherapy*, 2017.

[6] A. Potron, L. Poirel, and P. Nordmann, 'Emerging broad-spectrum resistance in Pseudomonas aeruginosa and Acinetobacter baumannii: Mechanisms and epidemiology', *International Journal of Antimicrobial Agents*. 2015.

[7] E. Tacconelli *et al.*, 'Discovery, research, and development of new antibiotics: The WHO priority list of antibiotic-resistant bacteria and tuberculosis', *Lancet Infect. Dis.*, vol. 18, no. March, 2017.

[8] G. Eskape, C. Drug, and T. Potential, 'Antibiotics Currently in Global Clinical Development', no. December 2017, 2018.

[9] S. Report, *SURVEILLANCE REPORT. Surveillance of antimicrobial resistance in Europe 2016*. 2017.

[10] A. J. Huh and Y. J. Kwon, '"Nanoantibiotics": A new paradigm for treating infectious diseases using nanomaterials in the antibiotics resistant era', *J. Control. Release*, vol. 156, no. 2, pp. 128–145, 2011.

[11] A. E. Clatworthy, E. Pierson, and D. T. Hung, 'Targeting virulence: A new paradigm for antimicrobial therapy', *Nat. Chem. Biol.*, vol. 3, no. 9, pp. 541–548, 2007.

[12] C. Grandclément, M. Tannières, S. Moréra, Y. Dessaux, and D. Faure, 'Quorum quenching: Role in nature and applied developments', *FEMS Microbiology Reviews*. 2015.

[13] S. Wagner *et al.*, 'Novel Strategies for the Treatment of Pseudomonas aeruginosa Infections', *J. Med. Chem.*, 2016.

[14] B. L. Angus, A. M. Carey, D. A. Caron, A. M. Kropinski, and R. E. Hancock, 'Outer membrane permeability in Pseudomonas aeruginosa: comparison of a wild-type with an antibiotic-supersusceptible mutant', *Antimicrob. Agents Chemother.*, 1982.

[15] T. Strateva and D. Yordanov, 'Pseudomonas aeruginosa – a phenomenon of bacterial resistance', no. 2009, pp. 1133–1148, 2019.

[16] H. P. Schweizer, 'Efflux as a mechanism of resistance to antimicrobials in Pseudomonas aeruginosa and related bacteria: Unanswered questions', in *Genetics and Molecular Research*, 2003.

[17] E. B. M. Breidenstein, C. de la Fuente-Núñez, and R. E. W. Hancock, 'Pseudomonas aeruginosa: All roads lead to resistance', *Trends in Microbiology*. 2011.

[18] G. P. Bodey, R. Bolivar, V. Fainstein, and L. Jadeja, 'Infections Caused by Pseudomonas aeruginosa', vol. 5, no. 2, pp. 279–313, 1983.

[19] a J. Morrison and R. P. Wenzel, 'Epidemiology of infections due to Pseudomonas aeruginosa.', *Rev. Infect. Dis.*, vol. 6 Suppl 3, no. October, pp. S627–S642, 2015.

[20] T. S. Murray, M. Egan, and B. I. Kazmierczak, 'Pseudomonas aeruginosa chronic colonization in cystic fibrosis patients', *Current Opinion in Pediatrics*. 2007.

[21] C. M. Waters and B. L. Bassler, 'QUORUM SENSING: Cell-to-Cell Communication in Bacteria', *Annu. Rev. Cell Dev. Biol.*, vol. 21, no. 1, pp. 319–346, 2005.

[22] J. Lee and L. Zhang, 'The hierarchy quorum sensing network in Pseudomonas aeruginosa', vol. 6, no. 1, pp. 26–41, 2015.

[23] C. Lu *et al.*, 'Discovery of antagonists of PqsR, a key player in 2-alkyl-4-quinolone- dependent quorum sensing in Pseudomonas aeruginosa', *Chem. Biol.*, 2012.

[24] M. Starkey *et al.*, 'Identification of Anti-virulence Compounds That Disrupt Quorum-Sensing Regulated Acute and Persistent Pathogenicity', *PLoS Pathog.*, vol. 10, no. 8, 2014.

[25] S. P. Diggle *et al.*, 'The Pseudomonas aeruginosa 4-Quinolone Signal Molecules HHQ and PQS Play Multifunctional Roles in Quorum Sensing and Iron Entrapment', *Chem. Biol.*, vol. 14, no. 1, pp. 87–96, 2007.

[26] G. Rampioni *et al.*, 'Unravelling the Genome-Wide Contributions of Specific 2-Alkyl-4-Quinolones and PqsE to Quorum Sensing in Pseudomonas aeruginosa', pp. 1–25, 2016.

[27] J. P. Coleman *et al.*, 'Pseudomonas aeruginosa PqsA is an anthranilate-coenzyme A ligase', *J. Bacteriol.*, vol. 190, no. 4, pp. 1247–1255, 2008.

[28] C. E. Dulcey, V. Dekimpe, D. Fauvelle, S. Milot, and U. Québec, 'NIH Public Access', vol. 20, no. 12, 2014.

[29] S. L. Drees and S. Fetzner, 'PqsE of Pseudomonas aeruginosa acts as pathway-specific thioesterase in the biosynthesis of alkylquinolone signaling molecules', *Chem. Biol.*, vol. 22, no. 5, pp. 611–618, 2015.

[30] A. F. Witzgall, T. Depke, M. Hoffmann, M. Brönstrup, R. Müller, and W. Blankenfeldt, 'Accepted Manuscript'.

[31] J. W. Schertzer, S. A. Brown, and M. Whiteley, 'Oxygen levels rapidly modulate Pseudomonas aeruginosa social behaviours via substrate limitation of PqsH', vol. 77, no. August, pp. 1527–1538, 2010.

[32] D. Maura *et al.*, 'Polypharmacology Approaches against the Pseudomonas aeruginosa MvfR Regulon and Their Application in Blocking Virulence and Antibiotic Tolerance', *ACS Chem. Biol.*, vol. 12, no. 5, pp. 1435–1443, 2017.

[33] S. Wagner *et al.*, 'Novel Strategies for the Treatment of Pseudomonas aeruginosa Infections', *J. Med. Chem.*, vol. 59, no. 13, pp. 5929–5969, 2016.

[34] F. Bredenbruch, R. Geffers, M. Nimtz, J. Buer, and S. Häussler, 'The Pseudomonas aeruginosa quinolone signal (PQS) has an iron-chelating activity', *Environ. Microbiol.*, vol. 8, no. 8, pp. 1318–1329, 2006.

[35] J. Lin, J. Cheng, Y. Wang, and X. Shen, 'The Pseudomonas Quinolone Signal (PQS): Not Just for Quorum Sensing Anymore', *Front. Cell. Infect. Microbiol.*, vol. 8, no. July, pp. 1–9, 2018.

[36] K. Kim, Y. U. Kim, B. H. Koh, S. Seok, and S. Kim, 'HHQ and PQS , two Pseudomonas aeruginosa quorum-sensing molecules , down-regulate the innate immune responses through the nuclear factor- j B pathway', pp. 578–588, 2010.

[37] C. Legendre, F. J. Reen, M. J. Mooij, G. P. Mcglacken, and C. Adams, 'Pseudomonas aeruginosa', vol. 80, no. 11, pp. 3985–3992, 2012.

[38] H. Ran, D. J. Hassett, and G. W. Lau, 'Human targets of Pseudomonas aeruginosa pyocyanin.', *Proc. Natl. Acad. Sci. U. S. A.*, vol. 100, no. 24, pp. 14315–20, 2003.

[39] C. C. Caldwell *et al.*, 'Pseudomonas aeruginosa exotoxin pyocyanin causes cystic fibrosis airway pathogenesis', *Am. J. Pathol.*, vol. 175, no. 6, pp. 2473–2488, 2009.

[40] L. G. Rahme, E. J. Stevens, S. F. Wolfort, J. Shao, R. G. Tompkins, and F. M. Ausubel, 'Common irulence factors for bacteial pathogenicity in plants and animals', *Science (80-.).*, vol. 268, no. June, p. 1899-, 1995.

[41] M. Kesarwani *et al.*, 'A quorum sensing regulated small volatile molecule reduces acute virulence and promotes chronic infection phenotypes', *PLoS Pathog.*, 2011.

[42] H. Cao, G. Krishnan, B. Goumnerov, J. Tsongalis, R. Tompkins, and L. G. Rahme, 'A quorum sensing-associated virulence gene of Pseudomonas aeruginosa encodes a LysR-like transcription regulator with a unique self-regulatory mechanism', *Proc. Natl. Acad. Sci.*, vol. 98, no. 25, pp. 14613–14618, 2001.

[43] S. E. Maddocks and P. C. F. Oyston, 'Structure and function of the LysR-type transcriptional regulator (LTTR) family proteins', *Microbiology*, vol. 154, no. 12, pp. 3609–3623, 2008.

[44] F. J. Reen, M. Barret, E. Fargier, M. O'Muinneacháin, and F. O'Gara, 'Molecular evolution of LysR-type transcriptional regulation in Pseudomonas aeruginosa', *Mol. Phylogenet. Evol.*, vol. 66, no. 3, pp. 1041–1049, 2013.

[45] K. Kefala, D. Kotsifaki, M. Providaki, E. G. Kapetaniou, L. Rahme, and M. Kokkinidis, 'Purification, crystallization and preliminary X-ray diffraction analysis of the C-terminal fragment of the MvfR protein from Pseudomonas aeruginosa', *Acta Crystallogr. Sect. F Struct. Biol. Cryst. Commun.*, vol. 68, no. 6, pp. 695–697, 2012.

[46] A. Ilangovan *et al.*, 'Structural Basis for Native Agonist and Synthetic Inhibitor Recognition by the Pseudomonas aeruginosa Quorum Sensing Regulator PqsR (MvfR)', *PLoS Pathog.*, vol. 9, no. 7, 2013.

[47] T. Kitao *et al.*, 'Molecular Insights into Function and Competitive Inhibition of *Pseudomonas aeruginosa* Multiple Virulence Factor Regulator', *MBio*, vol. 9, no. 1, pp. e02158-17, 2018.

[48] N. Xu, S. Yu, S. Moniot, M. Weyand, and W. Blankenfeldt, 'Crystallization and preliminary crystal structure analysis of the ligand-binding domain of PqsR (MvfR), the Pseudomonas quinolone signal (PQS) responsive quorum-sensing transcription factor of Pseudomonas aeruginosa', *Acta Crystallogr. Sect. F Struct. Biol. Cryst. Commun.*, vol. 68, no. 9, pp. 1034–1039, 2012.

[49] F. Soukarieh *et al.*, 'In silico and in vitro-guided identification of inhibitors of alkylquinolone-dependent quorum sensing in pseudomonas aeruginosa', *Molecules*, vol. 23, no. 2, 2018.

[50] T. Bjarnsholt *et al.*, 'Quorum sensing and virulence of Pseudomonas aeruginosa during lung infection of cystic fibrosis patients', *PLoS One*, vol. 5, no. 4, pp. 1–10, 2010.

[51] H. L. Barr *et al.*, 'Pseudomonas aeruginosa quorum sensing molecules correlate with clinical status in cystic fibrosis', *Eur. Respir. J.*, vol. 46, no. 4, pp. 1046–1054, 2015.

[52] H. L. Barr *et al.*, 'Diagnostic and prognostic significance of systemic alkyl quinolones for P. aeruginosa in cystic fibrosis: A longitudinal study', *J. Cyst. Fibros.*, vol. 16, no. 2, pp. 230–238, 2017.

Chapter 2

In silico identification and *in vitro* characterization of novel MvfR inhibitors

EXECUTIVE SUMMARY

M64 is a well-known MvfR inhibitor that can modulate the expression of MvfR without altering bacterial cell viability or growth. Moreover, it is able to inhibit the pathogenicity of Multi Drug Resistance (MDR) clinical isolates and reduce *P. aeruginosa* virulence in clinically mouse infection models. Despite of these suitable antivirulence characteristics, M64 is a high hydrophobic compound, thus some chemical efforts should be applied in order to improve solubility of the compound. Moreover, substitution of the nitro aromatic residue could be a possibility to decrease levels of mammalian cells cytotoxicity. Although M64 will not enter directly into clinical trials, it can acts as a template for the development of next generation of antivirulence compounds [1]**.** In order to search for novel inhibitors of MvfR protein a structure-based *in silico* screening approach was performed following docking studies on the previously published inhibitor, M64.

In addition, effect of selected compounds and its derivatives on phenotype assays such as virulence factors production (pyocyanin), on alkyl-quinolone signal molecules (HAQs) production and the interaction with the target by Surface Plasmon Resonance were assessed in order to characterize them for future pharmacodynamics evaluation.

MATERIALS AND METHODS

1. *IN SILICO* SCREENING

This part of the project has been developed by Computational Chemistry department of Aptuit (Verona).

The available X-ray structures of the MvfR apo-protein (PDB 4JVC) and complexes with the native agonist NHQ (PDB 4JVI) and a quinazolinone antagonist $3NH_2$-7Cl-C9 QZN, (PDB 4JVD) were loaded into MOE [2] and examined to identify key interaction binding site pharmacophore(s), useful to "drive" docking studies experiments on M64. Water analysis and electrostatic potential map calculations completed the binding pocket analysis. Conformational search of M64 structure (stochastic search, Force Field MMFF94x, Born generalized implicit solvent model, energy window 7 Kcal/mol) was first performed.

Docking experiments of the M64 low energy conformations previously obtained were run into the energy minimized protein structure, using an induced fit protocol (Amber10:EHT FF, R-field implicit solvent model) Highly scoring poses selected according ligand strain energy, binding energy and scoring function (GBVI/WSA dg kcal/mol) implemented within MOE, were submitted to a few run of Low Mode Molecular Dynamics simulations, resulting in the identification of the most likely ligand interactions models. A few structure-based pharmacophore queries were built on these refined docking poses adding protein pocket excluded volumes and used to search a 6M conformational data base of commercial compounds created in house.

2. BACTERIAL STRAIN

Unless stated otherwise, *Pseudomonas aeruginosa* PA14 was the bacterial strain selected as the reference strain for compounds profiling. *P. aeruginosa* PA14 is a multidrug resistance strain and it is considered as a clinical highly virulent reference strain. In general, prior to each experiment, inoculum size from frozen stocks in 5 mL of Luria-Bertani (LB; Sigma-Aldrich) using a 15-mL culture tubes 16 xs100mm round bottom (Pyrex™) were grown overnight at 37 °C, 240 rpm, and 45° inclined (Excella E24, New Brunswick Excella). These particular conditions allowed a consistent and reproducible expression of the different biomarkers of virulence.

3. PYOCYANIN QUANTIFICATION MICRO-METHOD

In order to select the most effective MvfR inhibitors a 96-deep well U-bottom MTP (VWR) based assay was used. An overnight culture of *P. aeruginosa* PA14 was appropriately diluted to an optical density of 0.04 ODU at 600 nm (OD_{600}, ~ $2\text{-}4x10^7$ CFU/mL) in fresh LB-Medium. 200 µl/well of bacterial suspension were dispensed in to the wells of the 96-deep-well MTP in the presence or absence of 100 µM NCEs to be screened. Compounds were prepared at 200 times the final concentration desirable in DMSO. 1 µl of each compound were dispensing in to the wells of the 96-deep-well-MTP (final concentration DMSO 0.5% v/v). The MvfR inhibitor M64 [1] was used as the reference standard compound for verifying assay performance and specificity. MTP was sealed using breathable tape sealer (Sigma-Aldrich) and incubated in a walk-in room for 24 h at 37 °C, under shaking (700 rpm, Delfie plate-shake, PerkinElmer). At the end of the incubation period, plates were centrifuged at 3,000 x g for 40 min at room temperature (RT). Finally, 100 µl of supernatant obtained were transferred to a new 96 well F-bottom MTP (VWR) and absorbance was determined at 690 nm (SPECTROstar

Nano BMG Labtech) Levels of pyocyanin production were expressed in terms of concentration (µM). Pyocyanin concentration was calculated using the following equation:

$$PYO\ Conc\ (M): \quad \frac{A690nm}{extinc\ coefficient\ (\varepsilon) * pathlengh\ (d)}$$

Where: A = A_{690} nm samples – A_{690} nm blank

ε = extinction coefficient (Pyo at A_{690} nm = 4,310 M^{-1} cm^{-1})

d = 0.23 cm (experimentally *d* for 100µl/well MTP F-Bottom)

Pyocyanin assay was performed only at 24 h since very low basal levels of pyocyanin were detected at 6 h in *P. aeruginosa* PA14 strain (< 20 µM).

4. LC-MS/MS HAQs MOLECULES QUANTIFICATION

An overnight PA14 culture was diluted in fresh LB to an optical density of 0.04 ODU at 600 nm (OD_{600}, ~ 2-4x10^7 CFU/mL). Then, 5 mL of bacteria suspension were dispensed in 15-mL culture tubes 16x100mm round bottom (Pyrex™) in the presence or absence of Compound **21**, Compound **97** and **M64**, as the reference compound. Hit compounds (**21** and **97**) were tested in a concentration range of 100 µM to 1.5 µM, whereas M64 (IC_{50} values of 200–350 nM for HHQ, PQS [1]) was tested from 31.6 µM to 0.03µM. 25 µl of each concentration was added to the tube containing the 5 mL bacterial culture (final concentration of DMSO 0.5% v/v) Levels of PQS and HHQ were measured at both 6 and 24 hours. The incubation was carried out at 37 °C, under shaking (300 rpm), and 90° inclination tubes (Excella E24, New Brunswick Ecella). The treatment of the samples after both time points was equal i.e., 0.5mL of MeOH containing 0.2 µg/mL D4-PQS, 0.4µg/mL D4-HHQ and 2% acetic acid was added to each vial containing 0.5 mL of sample and underwent vigorous agitation (Vortex Mixer ZX3, Uniequip). The vials

were then centrifuged at 12,000 x g for 5 min at 4 °C (Biofuge Fresco, Heraeus) and 200 µL of supernatant obtained were transferred to glass vials (Vial CRIMP 0.2 mL, VWR) and kept at -80 °C until LC-MS/MS analysis.
Analysis was carried out using an Agilent 1100 HPLC system and CTC PAL-HTS autosampler coupled with AB Sciex API4000 mass spectrometer. PQS (MW=259.34 g/mol) and HHQ (MW=243.34 g/mol) quantification was carried out using an optimized method based on LC-MS/MS analysis and the stable isotope dilution method [3]. The internal standard (IS) solution was prepared in MeOH with a final concentration of 200 ng/mL D4-PQS and 400 ng/mL D4-HHQ.
Biomarkers levels in the presence of different concentrations of M64/NCEs were expressed as percentage of inhibition of the basal levels in control samples. Curve fitting and IC_{50} estimations were carried out using a four parameter logistic model (GraphPad Prism v5).

5. CHEMICAL SYNTHESIS AND MODIFICATIONS

All the compounds were synthesized following the same procedure. In a 2-necked 25 mL round flask **a** (244 mg, 0.736 mmol), **b** (141 mg, 0.674 mmol), Py-BOP (427 mg, 0.82 mmol) were added and dissolved in dry DMF (7 mL). Finally, TEA (triethylamine) (0.107 mL, 0.77 mmol) was added and the yellow-orange solution was stirred at room temperature. After 20 h the reaction mixture was diluted with EtOAc (50 mL) and washed with NH_4Cl 1 M (2 x 50 mL). The yellow organic layer was dried (Na_2SO_4) and evaporated to an orange deliquescent solid. Silica gel column chromatography (SO_2; CHX/EtOAc 60:40 to 30:70) afforded product **c** as a pale-yellow solid (0.175 g, 0.335 mmol, 46%).

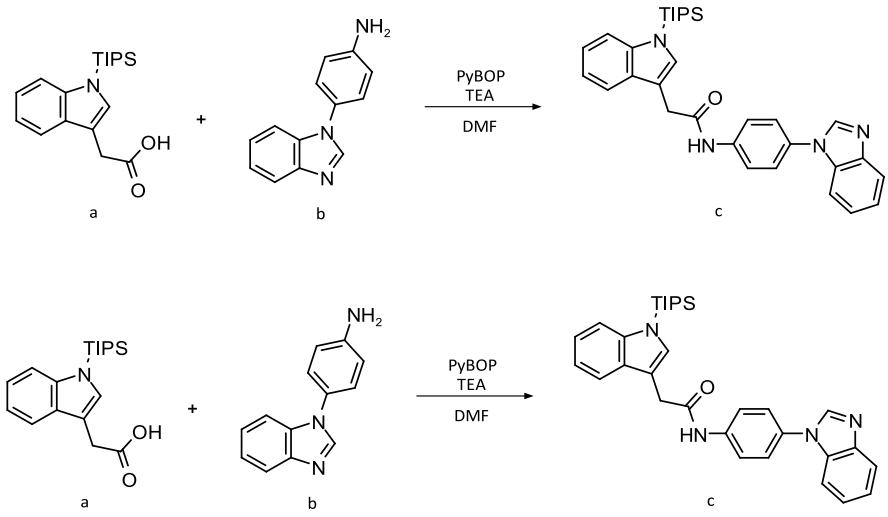

Figure 1. Organic synthesis process of compound **c**, previous step to obtain compound 21.

To a 25 mL round flask **c** (175 mg, 0.335 mmol) was dissolved in THF (3.0 mL) and TBAF (1 M in THF, 0.370 mL, 0.370 mmol) was added. After 10 minutes the mixture was diluted with EtOAc (30 mL) and washed with water (4 x 30 mL). The organic layer was dried (Na_2SO_4) and evaporated under reduced pressure to a colourless transparent solid.

Silica gel column chromatography (SiO_2, CHX/EtOAc 80:20 to 0:100) afforded product **21** as a white solid (0.112 g, 0.306 mmol, 91%).

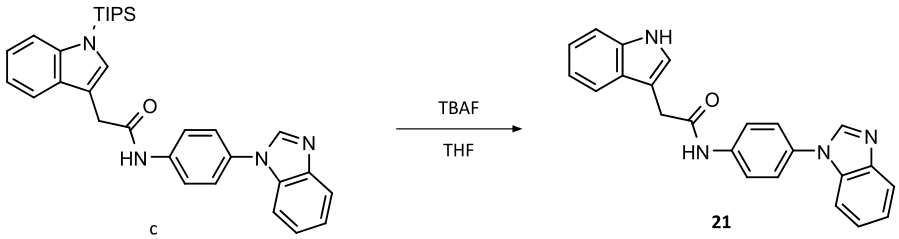

Figure 2. Final step on synthesis of compound 21.

6. DETERMINATION OF ANTIBIOTIC SUSCEPTIBILITY

Minimal Inhibitory Concentrations (MIC) was determined by the microdilution method according to the protocols recommended by the Clinical and Laboratory Standards Institute [4], with small modification; LB-Medium, as the main medium of all the experiments, was used instead of the recommended CAMHB.

7. EXPRESSION AND PURIFICATION OF MVFR^{LBD}

The gene fragment coding for MvfR^{LBD} (residues 91-332) was cloned, inserted into modified pMalC2X (NEB) i.e., insertion of a Hexa-His tag on the *N*-terminus of the vector-encoded MBP, and replacement of Factor Xa site with TEV site (University of Cambridge), and transformed into the competent cells *Escherichia coli* DH5α (Thermofisher). 3 mL of transformed bacteria overnight cultures containing MvfR^{LBD} was resuspended in 1L of LB medium supplemented with 2g of glucose and 50 µg/mL of carbenicillin. Cultures were grown with good aeration at 37 °C, 200 rpm to an optical density of 0.5-0.6 ODU at 600 nm. Following this, expression of the protein was induced by addition of IPTG (Sigma-Aldrich) 0.3 mM final concentration for 3 h. The cells were pelleted (10 min, 7500 x g, 4 °C) and resuspended in buffer A (Tris-HCl 50 mM, NaCl 5 M, 5% (v/v) Glycerol, EDTA 0.5 mM, DTT 1 mM) containing one pill of cOmplete^{TM}, Mini, EDTA-Free Protease Inhibitor Cocktail (Sigma-Aldrich). The cell suspension was lysed using a tip sonicator (2 cycles, 30 sec/cycle) and clarified by centrifugation (20 min, 25,000 x g, 4 °C). The clear supernatant was loaded onto an amylose column (NEB) equilibrated and washed overnight at 4 °C with buffer A. The fusion protein was eluted with a small volume of buffer A containing 10 mM maltose (without DTT and EDTA). Tev protease (Sigma-Aldrich) was added to the protein sample to cleave the MBP-tag during 18 h

on a roller at 4 °C. The mixture (His_6-MPD-tag + $MvfR^{LBD}$) was loaded onto a Ni-NTA column (NEB). A sufficient amount of soluble protein was obtained after the Ni-NTA purification column. The $MvfR^{LBD}$ pure protein was concentrated up to 1.5 mL using Vivaspin Column 5,000 MW (GE Healthcare). Concentration of final protein was measured using Nanodrop 1000 (Thermo Scientific).

8. SURFACE PLASMON RESONANCE (SPR)

The interactions between test compounds and $MvfR^{LBD}$ protein were analysed using a Biacore T200 (GE Healthcare). $MvfR^{LBD}$ protein 40 μg/mL in 10 mM sodium acetate buffer (pH 5.5) was covalently immobilized on a CM7 Series S sensor chip using an amine coupling reagent kit (GE Healthcare) at the range level of 3,000 to 5,000 response units (RU). Phosphate-buffered saline (PBS) was used as running buffer during protein immobilization. CM7 sensor chip surface was activated with the standardized amine coupling procedure using EDC/NHS deactivation of residual esters with 1 M ethanolamine hydrochloride pH 8.5 (GE Healthcare). A final wash step with HCl removes non-covalently bound material.

Steady-state (GE Healthcare) followed by coupling of the protein and affinity analyses were carried out in order to evaluate the strength of the binding. The value of the equilibrium dissociation constant (K_D) is obtained by fitting a plot of response at equilibrium (5 sec before the end of association extracted from the double-reference-corrected sensorgrams) against the concentration.

9. SUBCULTURING OF H27 SKIN FIBROBLAST CELL LINE AND CELLTITER-GLO® ASSAY PROTOCOL

Standard protocol for subcultering H27 was followed. Briefly, frozen cell stock was quickly thawed in a 37 °C water bath and the content was

transferred into 15 ml centrifugation tube containing 10 ml of cell culture medium. Tubes were centrifuge at 125 g for 7 min. The supernatant was discarded and cells were resuspended in 1 ml of cell culture medium. Cell suspension was transferred into a 25 cm^2 containing 7 ml of pre-warmed medium. The flask was incubated at 37 °C, 5% CO_2, 95% humidity. After incubation, the old medium was discarded by pouring into a beaker (or by suction). The cell monolayer was washed with 10 ml of 1xPBS. PBS was discarded after washing. 1 ml of TrypLE was added onto the washed cell monolayer and the flask was rotated to cover the monolayer with TrypLE. Flask was incubated at room temperature (RT) until the cells detach, usually ~4-5 min. Cells were examined using a microscope to ensure that all the cells were detached and floating. Fresh pre-warmed growth medium (6-12 ml) was added and the cells gentle pipetting in order to detach all the cells. Cell suspension was transferred into 15 ml centrifugation tube and the tube was centrifuged at 125 g for 7 min. The supernatant was discard and cells were resuspended with 1 ml of cell culture medium. 0.2-0.33 ml of cell suspension was transferred to new culture bottle containing 20 ml of pre-warmed medium. Usually the subculture ratio with Hs27 cells is 1:3/1:4 two times a week. Flask was incubated 37 °C, 5% CO_2, 95% humidity. Finally, Hs27 cells were seeding into a 96-well microplate for cytotoxicity assays. Cells were detached according to the procedure explained above. After centrifugation, cells were resuspended in 10 ml of cell culture medium. A 50 µl sample was taken to an Eppendorf tube for cell counting. The cells were counted by the Countess II cell counter (Thermofisher) following the manufacturer's instructions. Cells suspension was diluted with fresh medium until ~37,500 cells/mL density. 200 µl/well (~7 500 cells/well from ~37 500 cells/ml suspension) of the cell suspension were added to 96-well plate with a multichannel pipette. The 96-well-MTP was incubated at 37 °C, 5% CO_2, 95% humidity for 24 hours. Cytotoxicity assay was performed in the assay

medium with reduced amount of FBS and following Promega's CellTiter-Glo® assay protocol.

RESULTS

1. COMPOUND SELECTION FROM VIRTUAL SCREENING

The available X-ray $MvfR^{LBD}$ protein structures (PDB 4JVC, PDB 4JVI and 4JVD) were loaded into MOE [2] and the protein-ligand complexes were prepared (repairing, protonation, hydrogens addition and tethered energy minimisation). The structures were then overlapped (Figure 3) and the binding site was analysed including water analysis and electrostatic potential maps calculations (Figure 4). Ligands interactions were finally evaluated. The 3-NH_2-7Cl- C_9-QZN makes an H bond with Leu207 backbone while both agonist (NHQ) and antagonist (QZN) interact by weak H-pi bond with Tyr258. According to Ilangovan *et al*. studies [5], a conserved water molecule (H_2O 501) was also found to be stable in the water analysis of the present study (Figure 4) makes an H bond with Gln194 and was considered as part of the receptor in docking studies. All these keys interactions were hence used to drive docking experiments

Docking studies of M64

We first performed docking studies of M64, which is a MvfR-inhibitor characterized by a high LogP and a low solubility. Conformational search was run (stochastic, Merck Molecular Force Field (MMFF) 94X, Born implicit solvent, 7 Kcal/mol cut off) within MOE and low energy conformations were docked using an induced fit protocol. Poses were relaxed

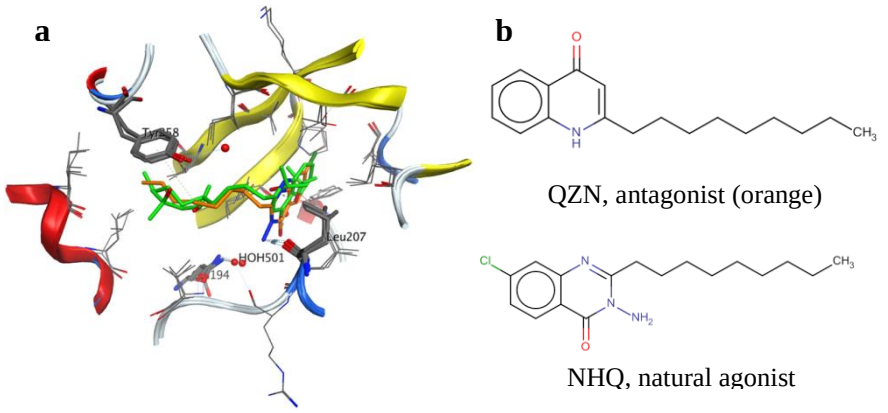

Figure 3. a) Overlapping of the MvfR^{LBD} agonist and antagonist complex X-ray structures. 3-NH_2-7Cl-C_9 QZN (orange) makes H bond with Leu207. Both agonist (green) and antagonist (orange) interact with Tyr258. Conserved water (H_2O 501) makes hydrogen bond with Gln194. b) Chemical structure of both antagonist and agonist.

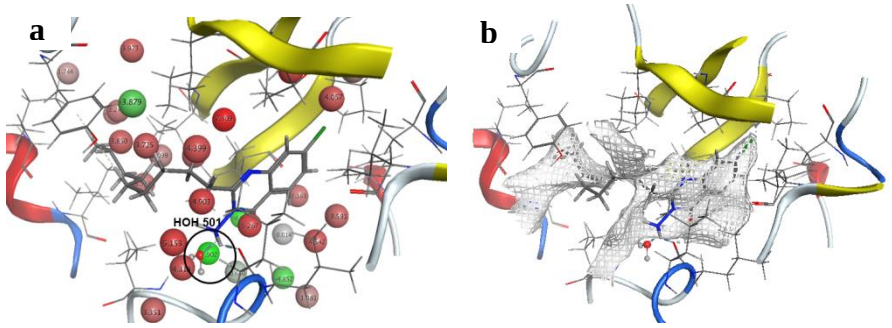

Figure 4. a)Water analysis run on of the X-ray MvfR^{LBD} of *Pseudomonas aeruginosa* with inhibitor 3NH_2-7Cl-C_9QZN (PDB 4JVI). Colour coded according to free energy: green (negative), white (zero) and red (positive).b) Hydrophobic electrostatic potential maps (-1.66Kcal/mol) of the X-ray MvfR^{LBD} *of Pseudomonas aeruginosa* with inhibitor 3NH_2-7Cl-C_9-QZN (PDB 4JVI). The extension of the map shows the lipophilic nature of the binding pocket

and scored using GBVI/WSA dG (Kcal/mol) scoring function. The top 5 poses were analysed and prioritised according to strain and binding energy.

As suspected, in the top scoring poses M64 is oriented in the binding site similarly as the ligands in the X-ray structures, making the same H bond with Leu207 in addition to others H bonds with Ile236 (donor) and Gln194 (acceptor). The M64 complex with the protein was further explored running a ligand-protein complex conformational search using Low Mode Molecular Dynamics (LMMD) method on a shell of 4.5A from the ligand atoms, tethering the ligand and the C alpha protein atoms. The ligand interactions pattern was confirmed, with an additional π-π stacking interaction of the M64 distal aromatic ring with Tyr258 (Figure 5).

A structure-based query was built using M64 best pose and the X-ray ligands, adding the shape of the binding pocket as protein excluded volumes (Figure 6).

The query was used to run pharmacophore search into a 6M in house 3D database of commercial compounds. A search with at least 6 features (out of 7) matched resulted in the identification of ~2.6K hits from which 141 compounds were finally selected applying drug-like physic-chemical filters [6] followed by structural clustering (0.78 cut off). Similarity to known MvfR inhibitors [1], [5] was also assessed and structures too similar to known ligands were rejected.

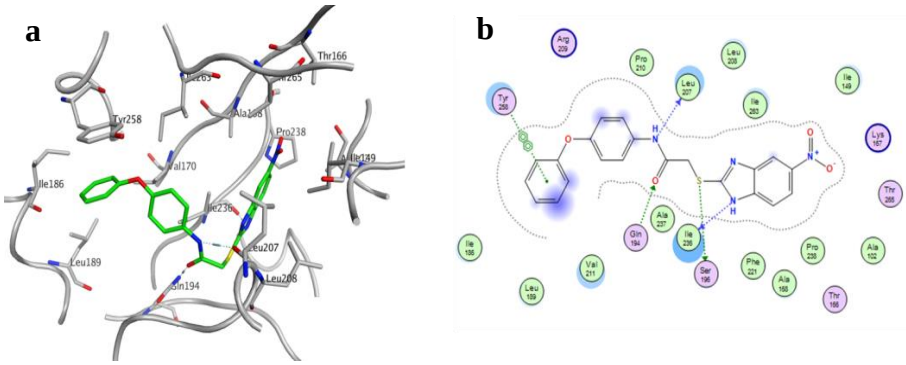

Figure 5. a) M64 best pose on MvfR ligand binding pocket. b) M64 interactions with residues within ~4.5A from the MvfR-inhibitor.

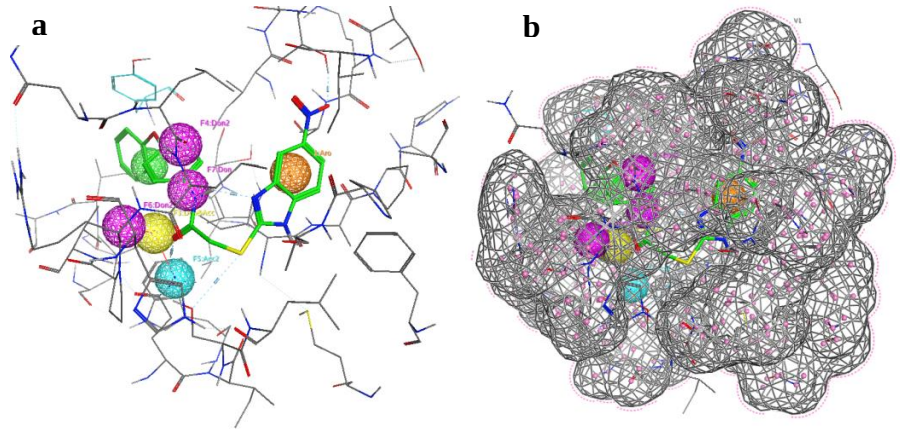

Figure 6. a) Pharmacophore query mapped on M64 best optimized pose. Features are colour coded: Cyan -Hydrogen Acceptor , purple -Hydrogen donor, orange -Aromatic , green - Hydrophobic , yellow - Donor & Acceptor . b) Pharmacophore query with excluded volumes

2. EFFECT OF SELECTED COMPOUNDS ON PYOCYACIN PRODUCTION

Pyocyanin is a blue-colored tricyclic phenazine, considered a secondary metabolite produced by *P. aeruginosa* during both acute and chronic infection. The production of pyocyanin is regulated, principally, by the MvfR QS system. Mutants in MvfR transcriptional factor did not produce pyocyanin and showed attenuation on its ability to infect and colonized mouse lungs in acute infections when compared with the wild type strain [7].

The initial hits were identified from 141 compounds selected from *in silico* screening model, by screening the compounds on *P. aeruginosa* PA14 pyocyanin production. We tested the effect of exposure 100 μM of each compound in a 96-deep-well MTP to *P. aeruginosa* culture. The results are expressed as % inhibition of pyocyanin production (Figure 8).

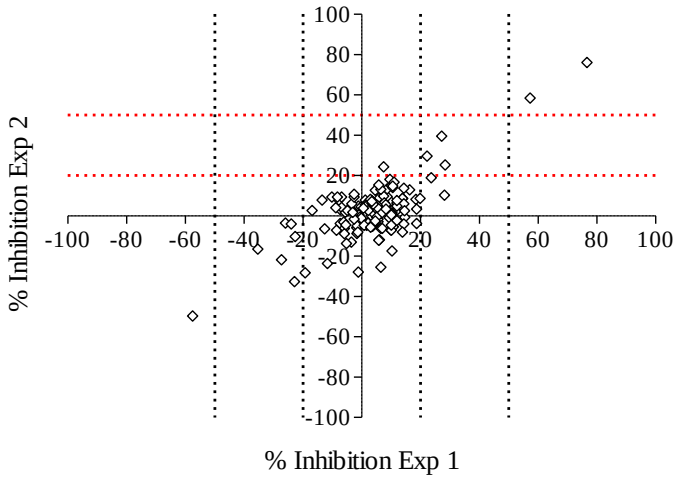

Figure 7. Pyocyanin % inhibition from two independent experiments (n=2) of 141 compounds selected from *in silico* screening. Diamond represents the mean of at least 3 replicates/compound/experiments.

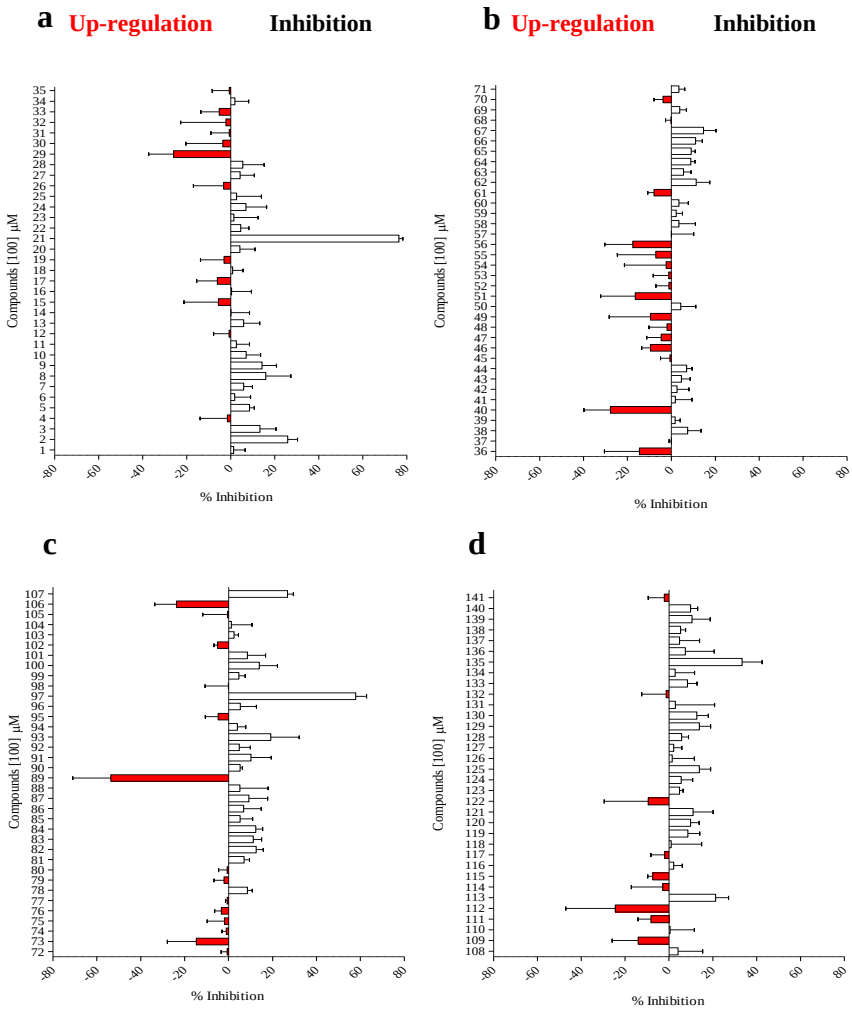

Figure 8. Pyocyanin production in presence of 100 µM of concentrations of 141 compounds. Red bars represent up- regulation of the MvfR activity (overproduction of pyocyanin) and white bars down- regulation (inhibition of pyocyanin).a) Compounds 1-35 b)Compounds 36-71 c) Compounds 72-107 d)Compounds 108-141. Error bars represent standard deviation of n=2 biological replicates.

Furthermore, the percentages of pyocyanin inhibition of two independently experiments were compared (Figure 7). 2 compounds showing more pyocyanin inhibition > 50% in two independent experiments (n=2) (1.41% hit-rate) were identified by this assay. In addition, 2.13% of the compounds showed an inhibition ranging between 20%-50% in the two independent experiments. 63.12% of compounds demonstrated less than 20% of inhibition. 33.33% of the compounds were able to up-regulate the MvfR, thus enhancing pyocyanin production (Figure 7 and Figure 8).

Compound **21** and compound **97,** the two most promising compounds, showed a pyocyanin inhibition of 76.38 % ± 1.76 and 57.86% ± 4.95 at 100 μM concentration (n=2), respectively.

No antibacterial activity against *P. aeruginosa* PA14 was found for both compounds up to the highest concentration tested (MIC > 128 μg/mL), as determined by the broth microdilution test, following CSLI guidelines with small modifications (LB medium).

3. EFFECT OF COMPOUND 21 AND 97 ON HAQs MOLECULES PRODUCTION

One class of quorum sensing molecules produced by *P. aeruginosa* is 4-hydroxy-2-alkylquinolones (HAQs), regulated via the PQS QS system. Among HAQs molecules, PQS and its precursor HHQ, are two of the most abundant molecules produced by this pathogen. These molecules act, in principle, as quorum sensing signal molecules. Both HHQ and PQS acts as co-inducing ligands of MvfR, the transcriptional regulator controlling *pqsABCDE* and *phnAB* operons. In order to evaluate MvfR activity and regulation in the presence or absence of the two selected hits, the HHQ and PQS levels produced by *P. aeruginosa* PA14 strain were measured using

LC/MS-MS method [3]. Compound **21** and compound **97** were tested in a concentration range of 100-1 μM at two time points, 6 and 24 hours.

Compound **21** showed significant reduction of PQS and HHQ production at 10 μM and 100 μM with respect to NT samples at both time points (6 and 24 hours). Percentage of inhibition at the highest concentration (100 μM) was calculated resulting in 53.1 % ± 3.24 PQS inhibition at 6 hours whereas at 24 hours a decline on PQS inhibition was observed until 20.28 % ± 0.28. Furthermore, 45.86 % ± 2.44 HHQ inhibition at the highest concentration (100 μM) was determined at 6 h and this effect remained overtime (55.63% ± 0.45 at 24h) (Figure 9).

On the other hand, compound **97** only showed significant PQS and HHQ reduction relative to NT samples at highest concentration tested (100 μM) at 6 hours. HAQs molecules were inhibited less than a 50% by compound **97** at both time points (Figure 10).

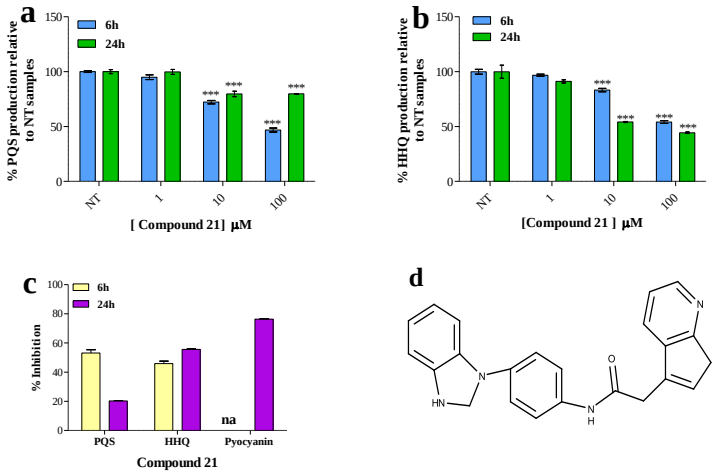

Figure 9. HAQs molecules produced by *P. aeruginosa* PA14 in presence of compound **21** at different concentrations (1, 10 and 100 µM). a) % PQS production relative to NT samples. b) % HHQ production relative to NT samples. The bars show percentage levels in relation to non-treated sample. Error bars represented the standard deviation of n=4 biological replicates. Statistical significant was assessed using Oneway ANOVA analysis followed by Dunnet's post-test. c) Inhibition of HAQs at 6 h (yellow bars) and 24 h (violet bars) and pyocyanin production in presence of 100 µM compound **21**. Not available (na) data for pyocyanin production at 6h. d) Compound **21** chemical structure.

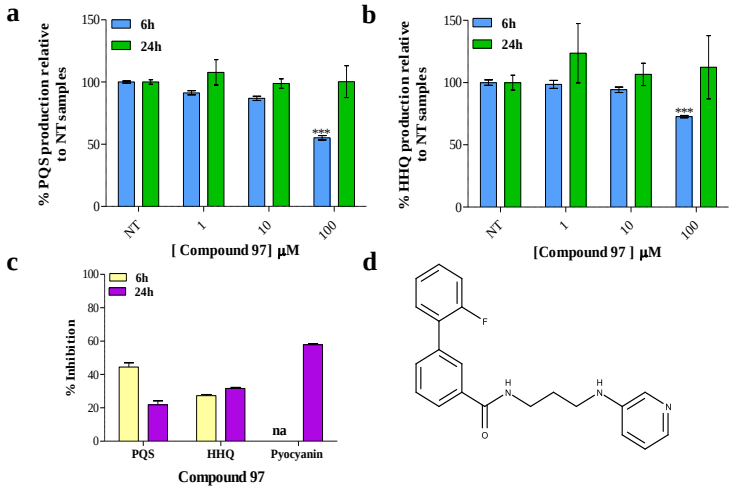

Figure 10. HAQs molecules produced by *P. aeruginosa* PA14 in presence of compound **97** at different concentrations (1, 10 and 100 µM). a) % PQS production relative to NT samples. b) % HHQ production relative to NT samples. The bars show percentage levels in relation to non-treated sample. Error bars represented the standard deviation of n=4 biological replicates. Statistical significant was assessed using Oneway ANOVA followed by Dunnet's post-test. c) Inhibition of HAQs at 6 h (yellow bars) and 24 h (violet bars) and pyocyanin production in presence of 100 µM compound **97**. Not available (na) data for pyocyanin at 6h. d) Compound **97** chemical structure.

4. ANALOGUES OF COMPOUND 21

Organic synthesis plays an important role in the development of novel drugs. Chemical modifications on the active molecules may result in an increase, decrease or modification of the biological response.

After the identification of compound **21** as a preliminary novel MvfR-regulon inhibitor, small medicinal chemistry modifications were carried out in order to make the compound more "*drug-like*". From compound **21** we have obtained 6 analogues (Figure 11).

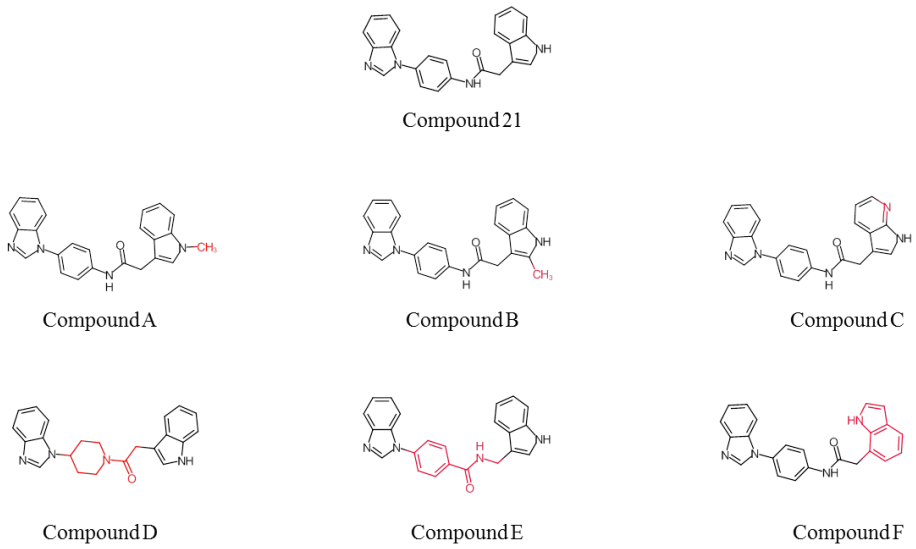

Figure 11.Chemical structure of compound 21 MvfR-regulon inhibitor and its 6 analogues. Medicinal chemistry modifications on compound 21 core structure are highlighted in red.

More in detail, Compound **A**, **B, C** and **F** were modified over indole group: adding methyl group at position 1, adding a methyl group at position 2, change the indole group to an azaindole group or changing the binding position from 3 to 4, respectively. On the other hand, the linker of compound **21** (anilide group) was changed to acetylpiperidine in the case of compound **D** and to benzamide group for compound **E**. All the analogues of compound **21** were obtained with purity between 97-99% and the reaction process

showed a really good yield (90-93%). Chemical characterization of all the compounds was successfully performed (Supplementary information).

5. IMPACT OF COMPOUND 21 ANALOGUES ON PYOACYNIN AND HAQs MOLECULES PRODUCTION

The six new MvfR-regulon inhibitors compounds were tested in order to evaluate the medicinal chemistry modifications in terms of biological responds. Phenotype pyocyanin assays were first performed, (Figure 13) following with the LC/MS-MS HAQs molecule assay. Modifications on linker of the molecule **21** (compound **D** and **E**), keeping intact the benzamidazol (LHS) and indole group (RHS) of the molecule neither show significant difference between the not treated (NT) samples in terms of pyocyanin nor in termns of HHQ/PQS production molecules at 24 h. Practically, *P. aeruginosa PA14* strain produced the same pyocyanin levels and HHQ/PQS signal molecules in presence of compound **D** and **E**. Moreover, either the addition of methyl group in the position 1 of the indole group (compound **B**) has presented a reduction on both pyocyanin and HAQs levels. However, compounds **A**, **C**, and **F**, which suffered small variations on indole group, seems to maintain the potency inhibitory activity observed in compound **21** regarding pyocyanin production. However, only compound **C**, showed greater inhibition than compound **21** for pyocyanin and HHQ/PQS levels. IC_{50} curves for PQS and HHQ were assessed for compound **21** and compound **C** (Figure 12). Nevertheless, only IC_{50} values could be calculated for compound **C**, with IC_{50} values of 47.89 µM for PQS and 39.9 µM for HHQ. In any case, at the highest concentration tested, compound 21 showed 40.9% inhibition of PQS and 52.9% inhibition of HHQ level. Compound C was confirmed to be the most promising compound among the derivatives synthesised.

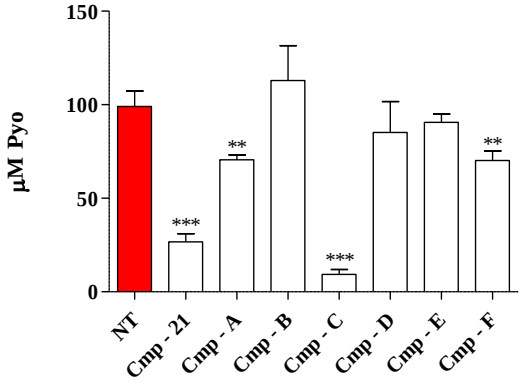

Figure 13. Pyocyanin levels in presence of 100 µM inhibitors. Error bars shows mean ± SD of 4 replicates. Difference between Not Treated (NT) PA14 and the samples in presence of compound 21, A, C and F was statistically significant (Oneway ANOVA, Dunnett's test).

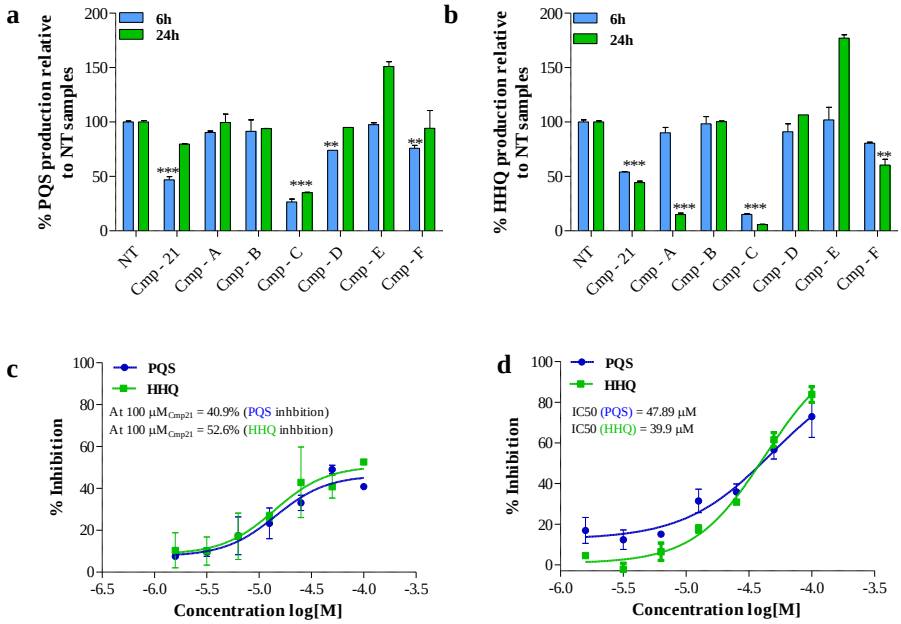

Figure 12. Relative production of a) PQS and b) HHQ in PA14 in presence of 100 µM compounds **21** and analogues at 6h (blue bars) and 24h (green bars) with respect to NT samples. The bars show mean±SD of percentage levels in relation to non-treated (NT) samples of at least 3 replicates. Statistical significant was assessed using Oneway analysis of variance (ANOVA) plus Dunnet's post-test. c) IC_{50} curve for compound **21**. d) IC_{50} curve for compound **C**.

6. SPR- BINDING EXPERIMENTS – STEADY STATE AFFINITY ANALYSIS

Surface Plasmon Resonance is a sensitive label-free method that allows the study of interactions between proteins and other molecules, an important step in the discovery and selection of molecules with the appropriate profile.

The MvfR protein is a LysR family transcriptional regulator that characteristically consists of an N-terminal helix-turn-helix (HTH) DNA-binding domain and a C-terminal ligand binding domain. The full length MvfR protein is showed to be very insoluble due to the HTH domain, therefore no crystal structure of the full length MvfR to date is available [8]. However, the ligand biding domain of MvfR has been described by many authors [5], [9]–[11]. Ilangovan *et al*. describes the binding pocket as two subdomains (CBDs I and II) connected by an antiparallel β-sheet termed the hinge region.

In this study, $MvfR^{LBD}$ (27.2 kDa) which is a soluble C-terminal fragment of 241 residues (from 91 to 332) was successfully purified (Supplementary information, Figure S 2) in order to carry out binding experiments using Steady State Affinity Analysis for the equilibrium dissociation constant (K_D) determination of the new MvfR-regulon inhibitors previously characterized. This part is needed to verify hits and discard false positives.

Compound **21** and its analogues were tested at different concentrations ranged 100µM-1.56 µM. K_D value was obtained by fitting a plot of response units (RU) at equilibrium against the compound concentrations tested. Steady state affinity measures are not affected by mass transport limitations since they are based on the report points taken at equilibrium.

The $MvfR^{LBD}$ was successfully immobilized (5815.8 RU) on the surface CM7 chip handling 40 µg/mL $MvfR^{LBD}$ in 10 mM Acetate pH 5.5. Sensorgrams demonstrated dose-response dependence for all the compounds

(Supplementary information, Figure S 1). The results of K_D are showed in Table 1.

Initial medicinal chemistry exploration on Compound **21** (K_D= 66.84 µM ± 7.02) led to a better interaction with the protein binding site (K_D = 28.73µM ± 1.12 for compound **C**) (Figure 14), which translated into a higher inhibitory pattern as demonstrated by pyocyanin and HHQ/PQS inhibition data. However, the interaction of compound **21** and **C** were 393 and 169 fold lower than M64 (K_D=0.17 µM ± 0.01), respectively (Table 1).

7. CELL VIABILITY ASSAYS - CYTOTOXICITY

Compounds were evaluated for their selectivity against mammalian cell lines. The viability human foreskin fibroblast line Hs27 cells was quantified using CellTiter-Glo® Luminescent Cell Viability Assay which is a homogeneous method of determining the number of viable cells in culture based on quantitation of the ATP present, which signals the presence of metabolically active cells. The homogeneous "add-mix-measure" format results in cell lysis and generation of a luminescent signal proportional to the amount of ATP present, which is further directly proportional to the number of cells present in the culture. The measurement of ATP content is based on luciferase reaction. The CellTiter-Glo® Assay generates a "glow-type" luminescent signal, which has a half-life of greater than five hours.

Compounds	K_D (µM)	R_{max}
M64	0.17 ± 0.01	61.84 ± 1.19
Cmp - 21	**66.84 ± 7.02**	74.435 ± 7.40
Cmp - A	72.41 ± 46.10	57.675 ± 26.38
Cmp - B	61.76 ± 17.66	50.47 ± 4.88
Cmp - C	**28.73 ± 1.12**	86.485 ± 3.68
Cmp - D	127.45 ± 15.91	83.6 ± 5.46
Cmp - E	179.00 ± 40.30	60.83 ± 11.72
Cmp - F	54.09 ± 4.72	77.715 ± 2.40

Table 1. Steady- State Affinity Analysis between MvfR- regulon inhibitors and $MvfR^{LBD}$. The mean of equilibrium constant dissociation (K_D) is expressed in µM concentrations units ±SD (n=2 replicates).

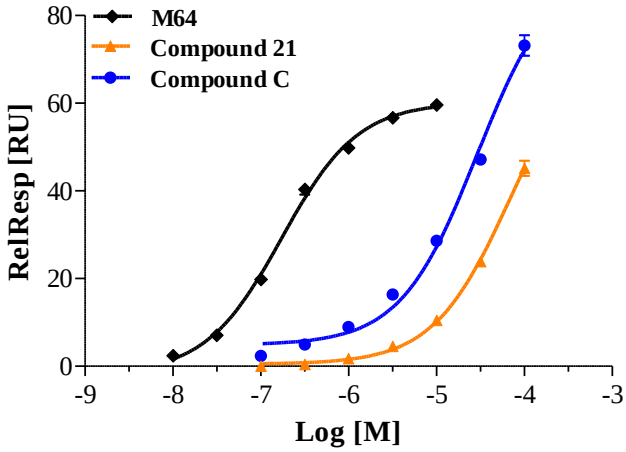

Figure 14. SPR Binding Experiments using Steady State Affinity Analysis of **M64** (Black), compound **21** (orange) and compound **C** (blue). Mean values of RU are represented. Error bars show as SD of two independently experiments (n=2).

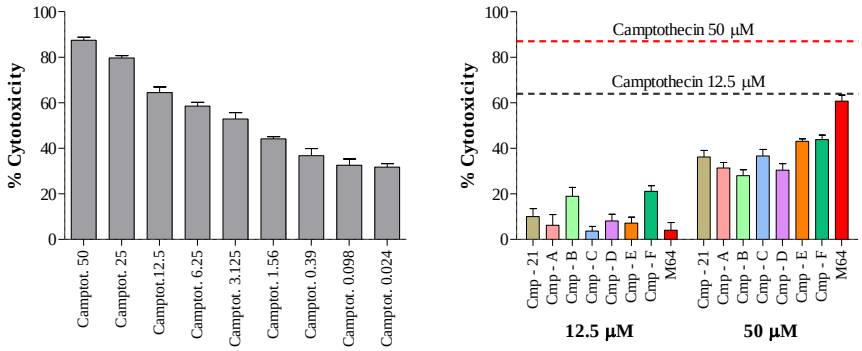

Figure 15. Determination of cytotoxicity against mammalian cells (Hs27) by using CellTiter-Glo® Luminescent Cell Viability Assay. Bars represent the % average cytotoxicity at two concentrations: 12.5 and 50 µM. Error bars represent the SD of replicates (n=3). Dashed lines represent the % cytotoxicity of the reference Camptothecin at both 12.5 µM (black dashed line) and 50 µM (red dashed line).

Compound **21** and its analogues show less than 20% of cytotoxicity at concentration of 12.5 µM. However, the cytotoxic effect increased with when compound concentration was doubled (50µM) (Figure 15). By contrast compound C, at 12.5 µM, showed the lowest % of cytotoxicity with repsect to the parent compound **21**.

DISCUSSION

Drug resistant bacteria are a global public health threat that is getting worse [12]. New approaches to antimicrobial drug discovery are currently needed to combat infections caused by these "superbugs". In the last priority list of antibiotic-resistant pathogens requiring urgent attention suggested by World Health Organization (WHO), *P. aeruginosa* ranked at second position because of its multidrug resistance to a broad spectrum of antibiotics including carbapenems and third generation of cephalosporin [12]. Hence, there is a pressing need for new classes of antibacterial agents with novel modes of action to combat *P. aeruginosa.* This Gram-negative bacterium is a

common cause of nosocomial infections and a major pathogen in immunocompromised individuals, above all in cystic fibrosis patients [13]. The clinical significance *of P. aeruginosa* emerges from its ability of produce different virulence factors during both acute and chronic infection [14]. Hence, quorum sensing system has been proposed as a potential target to disrupt bacterial communication with the objective of blocking virulence factors and auto-inducers molecules necessary for the acute and/or chronic infection thus inducing a chemical attenuation of pathogenicity without perturbing cell viability to minimizing the selective pressure that lead to the emergence of resistance [15].

P. aeruginosa possess four main quorum sensing systems, las, rhl, pqs and iqs that are interconnected to each other. It has been demonstrated that inhibitors of las and rhl QS systems have *in vitro* and *in vivo* anti-virulence potential [16], [17]. However, many studies describes the occurrence of *las* and *rhl* mutants in clinical *P. aeruginosa* isolates from CF chronic infections, hence further significance and clinical applicability for MvfR inhibitors [18].

The work done has been focussing on the design and characterization of novel inhibitors of the MvfR regulon. To date, a limited number of MvfR inhibitors were found [5], [19]–[21]. Some of them are structural analogues of anthranilic acid or PQS and HHQ analogues. However, it has been reported that *P. aeruginosa* is able to modify ligand-based MvfR inhibitors into MvfR activators, so drugs similar to anthranilic acid, PQS or HHQ are not the best candidates as MvfR inhibitors [22].

Based on the above and with the objective to find novel modulators of MvfR, we selected the M64 containing a structural backbone of a benzamide–benzamidazole (BB), which is far different from ligand-based MvfR inhibitors [1]. Moreover, M64 has been shown to be able to inhibit the pathogenicity of MDR clinical isolates and to reduce *P. aeruginosa* virulence in pre-clinical mouse infection models [1].

Key interactions between the $MvfR^{LBD}$ and the antagonist QZN showed by Ilagovan *et al*, as well as docking studies and ligand protein conformational search of $MvfR^{LBD}$-M64 complex carried out on the present study, allowed us building a structure-based query which was used to run pharmacophore search into a 6M in house 3D database of commercial compounds. The identification of 2,6K hits were achieve from which 141 compounds were finally selected applying drug-like physic-chemical filters followed by structural clustering.

The 141 compounds were screened in order to confirm pyocyanin production inhibition in *P. aeruginosa* PA14, considered as a good bacterial model because of its high virulence in humans. This phenotypic-based screening assay revealed that compound **21** with 76.38 % ± 1.76 percentage of inhibition were the most effective at reducing phenazine production, followed by compound **97** with 57.86% ± 4.95 of inhibition.

In full agreement with pyocyanin inhibition data, compound **21** exerted the most potent inhibitory activity on HAQs molecules production, whereas compound **97** showed only modest and variable effects on HAQs molecules levels. Based on the results obtained, some small medicinal chemistry modifications were carried out on compound **21** in order to attempt improvement activity. compound **C**, which was chemical modified by changing the indole group to an azaindole group, was the only derivative characterized by a higher *in vitro* activity in comparison with compound **21,** both in terms of pyocyanin (90.14% inhibition) and HAQs molecules production (IC_{50} values of 47.89 µM and 39.9 µM for PQS and HHQ, respectively).

Data from the SPR-based assay confirmed that the medicinal chemistry modifications, generating compound **C**, led to a 2 fold increase in binding affinity to the target (K_D = 28.73µM ± 1.12 for compound **C** *vs*. K_D= 66.84 µM ± 7.02 for compound **21**).

Despite that, compound **C** showed only activity at high µM range and lower inhibitory activity compared to MvfR quorum sensing inhibitors described in the literature [21].

The ideal MvfR quorum sensing inhibitors to treat bacterial infections in humans should be highly specific to the MvfR regulon, should disrupt bacterial communication in order to blocking virulence factors, such as pyocyanin, and autoinducers such as HHQ and PQS molecules without perturbing cell viability and should be non-toxic to mammalian cells. Thus, the tailored screening cascade develop and validate in this study could be proposed as a standard methodology for identification of NCEs targeting the MvfR regulon.

Most of the pyocyanin quantification studies to data, still used chloroform/HCl extraction from liquid cultures [23]. In the present study we proposed a HTP screening pyocyanin assay in a 96-deep-well plate in order to speed up the identification of novel MvfR inhibitors as a preliminary screening. The selection of most promising MvfR inhibitors compounds using a fast, accurate, sensitive, easy and economic assay is now possible.

In order to confirm functional effect on MvfR regulator, LC-MS/MS HAQs molecule assay was carried out, allowing calculating IC_{50} values for the main MvfR ligands, PQS and HHQ.

Moreover, in order to evaluate if the NCEs interact with the MvfR regulon protein, binding experiments (Steady State Affinity Analysis) using Surface Plasmon Resonance principle was set up for the purified $MvfR^{LBD}$ (241 residues). This technique allows real-time and label-free detection of biomolecular interactions in a short time [24]. This part is needed to verify hits and discard false positives from the phenotypes assays.

The Minimal Inhibitory Concentration assay is also a key point on the assay cascade, since one of the principal features of MvfR inhibitors is not disturb viability growth in order to minimize selective resistance bacteria.

All the steps followed in this study overcome the evaluation of the ideal characteristics for the identification of novel MvfR inhibitors.

SUPLEMENTARY INFORMATION

Chemical characterization of compound 21 and 6 analogues. NMR and MS ES are showed.

Compound 21: **^{1}H NMR** (400 MHz, DMSO) δ 10.93 (s, 1H), 10.36 (s, 1H), 8.48 (s, 1H), 7.85 (d, *J*= 8.8 Hz, 2H), 7.76 (dd, *J*=6.3, 2.3 Hz, 1H), 7.69-7.52 (m, 4H), 7.43-7.20 (m, 4H), 7.08 (t, *J*=7.3 Hz, 1H), 7.00 (t, *J*=7.4 Hz, 1H), 3.78 (s, 2H). **MS ES**+ (*m/z*): 367.43 (calc. for $C_{23}H_{19}N_4O$), 367.29 (found).

Compound A: ^{1}H NMR (400 MHz, MeOD) δ 8.36 (s, 1H), 7.83 (d, *J*= 8.7 Hz, 2H), 7.79-7.71 (m, 1H), 7.63 (d, *J*= 7.9 Hz, 1H), 7.56 (d, *J*= 8.5 Hz, 3H), 7.36 (dd, *J*= 8.2, 4.8 Hz, 3H), 7.19 (t, *J*= 7.3 Hz, 2H), 7.07 (t, *J*= 7.6 Hz, 1H), 3.86 (s, 2H), 3.81 (s, 3H). **MS ES+** (*m/z*): 381.46 (calc. for $C_{24}H_{21}N_4O^+$), 381.28 (found).

Compound B: **^{1}H NMR** (400 MHz, DMSO) δ 10.83 (s, 1H), 10.31 (s, 1H), 8.48 (s, 1H), 7.89-7.81 (m, 2H), 7.78-7.73 (m, 1H), 7.64-7.50 (m, 4H), 7.35-7.20 (m, 3H), 6.96 (dtd, *J*= 14.7, 7.1, 1.2 Hz, 2H), 3.72 (s, 2H), 2.41 (s, 3H). **MS ES**+ (*m/z*): 381.46 (calc. for $C_{24}H_{21}N_4O^+$), 381.31 (found).

Compound C: ^{1}H NMR (400 MHz, Acetone) δ 10.54 (s, 1H), 9.46 (s, 1H), 8.26 (s, 1H), 8.24 (dd, *J*=4.7, 1.5 Hz, 1H), 8.07 (dd, *J*=7.9, 1.5 Hz, 1H), 7.94-7.86 (m, 2H), 7.78-7.69 (m, 1H), 7.60-7.51 (m, 3H), 7.48 (s, 1H), 7.35-7.24 (m, 2H), 7.07 (dd, *J*= 7.9, 4.7 Hz, 1H) 3.89 (s, 2H).**MS ES**+ (*m/z*): 368.42 (calc. for $C_{22}H_{18}N_5O^+$), 368.27 (found).

Compound D: ^{1}H NMR (400 MHz, Acetone) δ 10.13 (s, 1H), 7.73 (d, *J*= 7.9 Hz, 1H), 7.51 (d, *J*= 7.9 Hz, 1H), 7.73 (dd, *J*= 16.0, 8.2 Hz, 2H), 7.33-7.27 (m, 1H), 7.19-7.11 (m, 1H), 7.11-7.02 (m, 3H), 7.02-6.94 (m, 1H), 6.39 (d, *J*= 3.2 Hz, 1H), 4.81 (d, *J*= 13.4 Hz, 1H), 4.60 (tt, *J*= 11.9, 4.1 Hz, 1H), 4.30 (d, *J*= 13.8 Hz, 1H), 3.93 (q, *J*= 14.9 Hz, 3H), 3.26 (t, *J*= 12.3 Hz, 1H), 2.77 (dd, *J*= 11.0, 10.1 Hz, 2H), 1.93-1.71 (m, 2H), 1.60-1.43 (m, 1H). **MS ES**+ (*m/z*): 358.46 (calc. for $C_{23}H_{24}N_3O^+$), 358.31 (found).

Compound E: **^{1}H NMR** (400 MHz, Acetone) δ 10.14 (s, 1H), 8.39 (s, 1H), 8.25-8.16 (m, 2H), 8.09 (s, 1H), 7.79-7.70 (m, 4H), 7.69-7.62 (m, 1H), 7.43-7.37 (m, 2H), 7.37-7.28 (m, 2H), 7.12 (ddd, *J*= 8.2, 7.1, 1.1 Hz, 1H), 7.03

(ddd, *J*= 8.0, 7.1, 1.0 Hz, 1H), 4.83 (dd, *J*= 5.5, 0.5 Hz, 2H).**MS ES+** (*m/z*): 367.43 (calc. for $C_{23}H_{19}N_4O^+$), 367.26 (found).

Compound F: **^{1}H NMR** (400 MHz, MeOD) δ 8.36 (s, 1H), 7.79-7.87 (m, 2H), 7.70-7.78 (m, 1H), 7.51-7.60 (m, 3H), 7.30-7.40 (m, 3H), 7.26 (d, *J*= 3.26 Hz, 1H), 7.07-7.15 (m, 1H), 7.00-7.06 (m, 1H), 6.62 (dd, *J*= 3.26, 0.75 Hz, 1H), 4.01 (s, 2H). **MS ES+** (*m/z*): 367.43 (calc. for $C_{23}H_{19}N_4O^+$), 367.27 (found).

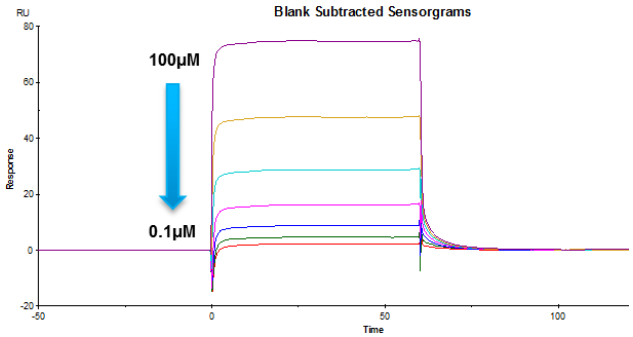

Figure S 1. Sensogram as an example of dose-response dependence from Steady-State Affinity Analysis between compound 21 and MvfR^{LBD} Response units *vs* time in seconds. Concentrations of compound 21 range from 100µM to 1µM.

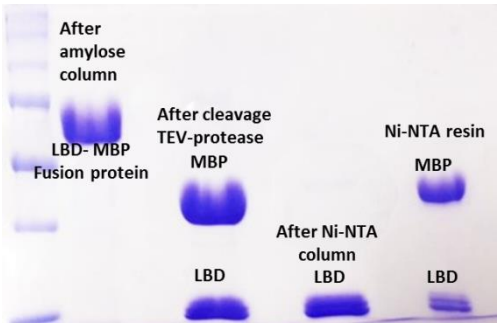

Figure S 2.Electrophoresis gel showing the products for the whole process of MvfR^{LBD} protein purification.

REFERENCES

[1] M. Starkey *et al.*, 'Identification of Anti-virulence Compounds That Disrupt Quorum-Sensing Regulated Acute and Persistent Pathogenicity', *PLoS Pathog.*, vol. 10, no. 8, 2014.

[2] 2013.08 Molecular Operating Environment (MOE), 'Molecular Operating Environment (MOE), 2013.08; Chemical Computing Group Inc., 1010 Sherbooke St. West, Suite #910, Montreal, QC, Canada, H3A 2R7.', *Mol. Oper. Environ. (MOE), 2013.08; Chem. Comput. Gr. Inc., 1010 Sherbooke St. West, Suite #910, Montr. QC, Canada, H3A 2R7, 2013.*, 2016.

[3] O. Albarbarawi, G. Devereux, and J. T. Huang, 'Characterization and validation of an isotope-dilution LC – MS / MS method for quantification of total desmosine and isodesmosine in plasma and serum', pp. 1991–2001, 1991.

[4] mlewis, 'M7-A7 - Methods for Dilution Antimicrobial Susceptibility Tests for Bacteria That Grow Aerobically; Approved Standard - Seventh Edition', no. January, pp. 1–64, 2005.

[5] A. Ilangovan *et al.*, 'Structural Basis for Native Agonist and Synthetic Inhibitor Recognition by the Pseudomonas aeruginosa Quorum Sensing Regulator PqsR (MvfR)', *PLoS Pathog.*, vol. 9, no. 7, 2013.

[6] C. A. Lipinski, 'Lead- and drug-like compounds: The rule-of-five revolution', *Drug Discovery Today: Technologies*. 2004.

[7] D. Mavrodi, 'Pseudomonas aeruginosa', *Society*, vol. 72, no. 7, pp. 4275–4278, 2004.

[8] K. Kefala, D. Kotsifaki, M. Providaki, E. G. Kapetaniou, L. Rahme, and M. Kokkinidis, 'Purification, crystallization and preliminary X-ray diffraction analysis of the C-terminal fragment of the MvfR protein from Pseudomonas aeruginosa', *Acta Crystallogr. Sect. F Struct. Biol. Cryst. Commun.*, 2012.

[9] K. Kefala, D. Kotsifaki, M. Providaki, E. G. Kapetaniou, L. Rahme, and M. Kokkinidis, 'Purification, crystallization and preliminary X-ray diffraction analysis of the C-terminal fragment of the MvfR protein from Pseudomonas aeruginosa', *Acta Crystallogr. Sect. F Struct. Biol. Cryst. Commun.*, vol. 68, no. 6, pp. 695–697, 2012.

[10] N. Xu, S. Yu, S. Moniot, M. Weyand, and W. Blankenfeldt, 'Crystallization and preliminary crystal structure analysis of the ligand-binding domain of PqsR (MvfR), the Pseudomonas quinolone signal (PQS) responsive quorum-sensing transcription factor of Pseudomonas aeruginosa', *Acta Crystallogr. Sect. F Struct. Biol. Cryst. Commun.*, vol. 68, no. 9, pp. 1034–1039, 2012.

[11] T. Kitao *et al.*, 'Molecular Insights into Function and Competitive Inhibition of *Pseudomonas aeruginosa* Multiple Virulence Factor Regulator', *MBio*, vol. 9, no. 1, pp. e02158-17, 2018.

[12] H. D. Marston, D. M. Dixon, J. M. Knisely, T. N. Palmore, and A. S. Fauci, 'Antimicrobial resistance', *JAMA - J. Am. Med. Assoc.*, vol. 316, no. 11, pp. 1193–1204, 2016.

[13] T. S. Murray, M. Egan, and B. I. Kazmierczak, 'Pseudomonas aeruginosa chronic colonization in cystic fibrosis patients', *Current Opinion in Pediatrics*. 2007.

[14] A. Crousilles *et al.*, 'Which microbial factors really are important in Pseudomonas aeruginosa infections?', *Future Microbiology*. 2015.

[15] C. M. Waters and B. L. Bassler, 'QUORUM SENSING: Cell-to-Cell Communication in Bacteria', *Annu. Rev. Cell Dev. Biol.*, 2005.

[16] D. A. Rasko and V. Sperandio, 'Anti-virulence strategies to combat bacteria-mediated disease', *Nature Reviews Drug Discovery*. 2010.

[17] J. Njoroge and V. Sperandio, 'Jamming bacterial communication: New approaches for the treatment of infectious diseases', *EMBO Molecular Medicine*. 2009.

[18] D. A. D'Argenio *et al.*, 'Growth phenotypes of Pseudomonas aeruginosa lasR mutants adapted to the airways of cystic fibrosis patients', *Mol. Microbiol.*, 2007.

[19] T. Klein *et al.*, 'Identification of small-molecule antagonists of the pseudomonas aeruginosa transcriptional regulator PqsR: Biophysically guided hit discovery and optimization', *ACS Chem. Biol.*, 2012.

[20] C. Lu *et al.*, 'Discovery of antagonists of PqsR, a key player in 2-alkyl-4-quinolone- dependent quorum sensing in Pseudomonas aeruginosa', *Chem. Biol.*, 2012.

[21] F. Soukarieh *et al.*, 'In silico and in vitro-guided identification of inhibitors of alkylquinolone-dependent quorum sensing in pseudomonas aeruginosa', *Molecules*, vol. 23, no. 2, 2018.

[22] C. Lu, C. K. Maurer, B. Kirsch, A. Steinbach, and R. W. Hartmann, 'Overcoming the unexpected functional inversion of a PqsR antagonist in Pseudomonas aeruginosa: An in vivo potent antivirulence agent targeting pqs quorum sensing', *Angew. Chemie - Int. Ed.*, 2014.

[23] P. V. Avizonis and J. C. Weiston, 'On the biosynthesis of felinine', *BBA - Biochim. Biophys. Acta*, vol. 34, no. C, pp. 279–281, 1959.

[24] K. S. Phillips and Q. J. Cheng, 'Surface plasmon resonance', in *Molecular Biomethods Handbook: Second Edition*, 2008.

Chapter 3

In vitro characterization of *P. aeruginosa* strains isolated from cystic fibrosis patients

EXECUTIVE SUMMARY

P. aeruginosa PAO1 and *P. aeruginosa* PA14 have been extensively used as the strains model in drug discovery. By contrast, it is of paramount importance, especially in the evaluation of quorum sensing modulators against a wider *P. aeruginosa* bacterial population, including those strains involved in cystic fibrosis.

A panel of 109 *P. aeruginosa* strains, received by Azienda Ospedaliera Universitaria Integrata di Verona (Centro Regionale Fibrosi Cistica), have been isolated from the sputum of patients affected by CF. A subpanel of 47 *P. aeruginosa* strains were selected in function of pyocyanin production and were fully characterised *in vitro* by measuring basal levels of pyocyanin, HAQs molecules and 2-AA pro-persistent molecule, as the most representative hallmarks of MvfR QS system. Additionally, biofilm formation and antimicrobial susceptibility profile were also assessed. The relationship between the different virulence factors, the clinical outcomes of the patient and the stage of infection referring to each of the *P. aeruginosa* strains, was also carried out.

The in depth characterization of this panel of strains allowed the identification of MDR *P. aeruginosa* ACC00901, as the isolate to be used for set-up and validation of chronic lung infection model in the rat, for the assessment of efficacy of the MvfR inhibitors identified through the screening cascade.

MATERIALS AND METHODS

1. CYSTICS FIBROSIS *P. AERUGINOSA* STRAINS

Under the collaboration with Azienda Ospedaliera Universitaria Integrata di Verona (Centro Regionale Fibrosi Cistica), a panel of 109 *P. aeruginosa* strains isolated from the sputum of 109 different cystic fibrosis patients in 2009 were received. The chronic pulmonary infection with *P. aeruginosa* in these patients was defined as >50% of cultures positive for *P. aeruginosa* in ≤12 months. All data associated to the strains are reported in Table 1S (Supplementary Information). The time of chronicity was calculated as the difference between year 2009 and the year when the patient was first positive for *P. aeruginosa.*

2. PYOCYANIN MEASUREMENTS – 24 hours production

Unless otherwise specified, prior to each experiment, inoculum from frozen glycerol stocks, was transferred in 5 mL of Luria-Bertani broth (LB; Sigma-Aldrich) using a 15-mL culture tubes 16 xs 100mm round bottom (Pyrex^{TM}), and grown overnight at 37 °C, 240 rpm, and 45° inclination (Excella E24, New Brunswick Excella). *P. aeruginosa* PA14 was used as reference laboratory strain.

Pyocyanin concentration was calculated as follow:

$$PYO\ Conc\ (M): \quad \frac{A690nm}{extinc\ coefficient\ (\varepsilon) * pathlengh\ (d)}$$

Where: A = A_{690} nm samples – A_{690} nm blank

ε = extinction coefficient (Pyo at A_{690} nm = 4,310 M^{-1} cm^{-1})

d = 0.23cm (experimentally *d* for 100µl/well MTP-F-Bottom)

Pyocyanin production 24 hours

Pyocyanin production was determined as follows. An overnight culture of the selected strain was diluted to an optical density of 0.04 ODU at 600 nm (OD_{600}, ~ 2-4x10^7 CFU/mL) with fresh LB-Medium. Then, 5 mL of bacteria suspension were dispensed into 16 x 100 mm round bottom 15-mL culture tubes (Pyrex™) and incubated at 37 °C, under shaking (240 rpm), and 45° inclination (Excella E24, New Brunswick Excella) during 24 hours. After the incubation, glass tubes were vortexed and 1 mL of the culture was transferred into a 1.5 mL Eppendorf. After centrifugation (8,000 g, 5 min, at room temperature, (RT) 100 µl of culture supernatant were transferred into a 96-well plate F-Bottom (VWR) and absorbance was determined at 690nm (SPECTROstar Nano). At least two replicates for each strain were assessed.
Based on the results obtained, a sub-population of 47 strains (Over the 109 strains tested) characterized referred as high pyocyanin producers (≥ 20 µM pyocyanin concentration detected at 24 h timepoint) was selected.

3. BIOFILM PRODUCTION ASSAY

P. aeruginosa PAO1 strain was used for this study as reference biofilm producer strain. PAO1 strain and CF isolates strains were streaked out from frozen glycerol stock over LB-agar plates (Sigma-Aldrich) and incubate overnight at 35 ± 2 °C. As starting inoculum, 0.5 McFarland (~1-2x10^8 CFU/mL) turbidity suspension was performed in saline solution (phosphate buffer saline (1x), Lonza) and then diluted 1:20 to achieve approximately ~1x10^6 CFU/mL bacterial cell suspension in fresh Tryptic Soy Broth (TSB) (Sigma-Aldrich) supplemented with 1% v/v of Glucose (1 M) (TSB^+). 160 µl/well were seed into a 96-well plate sterile U-bottom (VWR) in the presence of 0.5% v/v of DMSO (Sigma-Aldrich). Biofilm formation was carried out during 24 hours at 37 °C in static conditions. At the end of the

incubation period, the planktonic culture was removed from each well and rinse twice with 180 µl of Milli-Q sterile water (Millipore Corporation). The plates for bacterial challenge count were dried for 1 hour at room temperature (RT). 180 µl/well of 0.1 % Crystal Violet (CV) stain (Sigma-Aldrich) were added and incubation for 15 min was allowed. After incubation, CV was removed and the plate was rinsed once with 180 µl of Milli-Q sterile water and dried for 1 hour at RT. Then, 180 µl of Ethanol 96% (Sigma-Aldrich) were added into wells and incubation of 15 min followed. After incubation, 130 µl of the samples were transferred into a 96-well plate F-bottom (VWR) in order to measure the absorbance at 595nm (SPECTROstar Nano). The results obtained have been reported as mean ± SD. Low and high capability of forming biofilm was defined on the basis of absorbance values of the samples with respect to that of the reference – *low* = $OD_{PAO1} \geq OD_{sample}$, *high* = $OD_{PAO1} < OD_{sample}$.

At least 4 replicates per strains were included in the experiment.

4. LC-MS/MS HAQs MOLECULES AND 2-AA MOLECULE QUANTIFICATION

The CF isolates strains overnight culture was diluted to an optical density of 0.04 ODU at 600nm (OD_{600}, ~ 2-4x10^7 CFU/mL) in fresh LB. Then, 5 mL of bacteria suspension were dispensed in 16 x 100mm round bottom 15-mL culture tubes (3 internal replicates / strain) (Pyrex^{TM}) in the presence of 0.5% v/v DMSO (Sigma-Aldrich). Levels of PQS, HHQ and 2-AA were measured at two time-points, namely 6 and 24 hours. The incubation was carried out at 37 °C, 300 rpm 90° inclination (Excella E24, New Brunswick Excella). Irrespectively from the time-point considered, samples were processed with the same method. Briefly, 0.5mL of MeOH, containing 0.2 µg/mL D4-PQS, 0.4 µg/mL D4-HHQ and 2% acetic acid, was added to each vial containing

0.5 mL of sample and vortexed vigorously (Vortex Mixer ZX3, Uniequip). The vials were centrifuged at 4 °C, 12,000xg, for 5 min (Biofuge FRESCO, Heraeus) and 200 µl of the supernatant obtained was transferred to glass vials (Vial CRIMP 0.2mL, VWR), kept at -80 °C until LC-MS/MS analysis (Agilent 1100 HPLC system and CTC PAL-HTS autosampler coupled with AB Sciex API4000 mass spectrometer).

PQS (MW = 259.34 g/mol), HHQ (MW = 243.34 g/mol) and 2-AA (MW = 135.07 g/mol) quantification was carried out using an optimized method based on LC-MS/MS analysis and the stable isotope dilution quantification method [1]. The internal standard (IS) solution was prepared in MeOH with a final concentration of 200 ng/mL D4-PQS, 400 ng/mL D4-HHQ and 400 ng/ml D4-2AA

Results were expressed as ng/mL for each HAQs molecules and 2-AA.

LC/MS-MS analysis was performed by the DMPK Department of Aptuit (Verona) s.r.l.

5. ANTIBIOTIC RESISTANCE OF CF ISOLATES STRAINS

Antibiotic susceptibility profile of the cystic fibrosis isolates F was determined by the VITEK 2 System (BioMérieux). All the strains were streaked out from frozen stock over LB-agar plates (Sigma-Aldrich) and incubated overnight at 35 ± 2 °C. After incubation, a 0.5-0.6 McFarland turbidity suspension was prepared in saline solution - phosphate buffer saline (1x), Lonza. The specific Gram-negative card AST-N195 (BioMérieux) was used.

6. DETERMINATION OF KINETIC OF GROWTH

Growth curve of *P. aeruginosa* ACC00901 strains was carried out in Luria-Bertani Broth (LB, Sigma-Aldrich). One bead from MicroBank aliquot was

transferred to 10 mL of 100% LB and incubation was carried out at 35 ± 2 °C, overnight, under orbital shaking at 150 rpm. 1:1,000 dilution from the overnight culture was made with freshly prepared pre-warmed LB Broth and the new suspension was incubated at 35 ± 2 °C, under shaking (180 rpm) for 24 hours. Optical density at 600 nm, (SPECTROstar Nano,) was measured using 1 cm path-length cuvettes (Brand UV, Sigma-Aldrich) at time 0, time 2 and every hour until 8 hours. Colony forming unit (CFU) value was measured by traditional dilution methods at time 0, time 2 and then every hour until 8h and at 24 hours. Dilution was plated on LB-Agar plates (Sigma-Aldrich) and incubated at 35 ± 2 °C for 20-24 hours and the number of colonies was counted.

RESULTS

1. CLASSIFICATION OF 109 *P. AERUGINOSA* STRAINS IN FUNCTION OF PYOCYANIN PRODUCTION AT 24 HOURS

Substantial in vitro variability was found in pyocyanin production in the population of *P. aeruginosa* CF isolates considered. The blue/green phenazine concentration was determined quantitatively on supernatant from 24 hours cultures for all strains. This analysis led to the selection of 47 high producer strains (47.92%) (Figure 1), which have gone through the characterization reported in the next sections.

2. BIOFILM FORMATION

The 47 *P. aeruginosa* strains were classified as *low* ($OD_{PAO1} \geq ODs_{ample}$), or *high* ($OD_{PAO1} < OD_{sample}$) biofilm formers. A uniform distribution (*high*

biofilm formers 48.94% and *low* biofilm formers 51.06%) was observed over the 47 CF population strains (Figure 2).

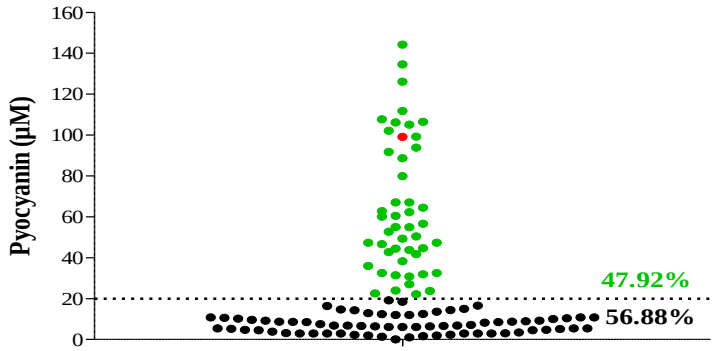

Figure 1. Pyocyanin 24 h basal levels of 109 *P. aeruginosa* CF strains. Pyocyanin concentration is expressed in µM. Classification of strains in function of pyocyanin production: strains producer < 20 µM (black dots), strains producers > 20 µM (green dots) and *P. aeruginosa* PA14 reference strain (red dot).

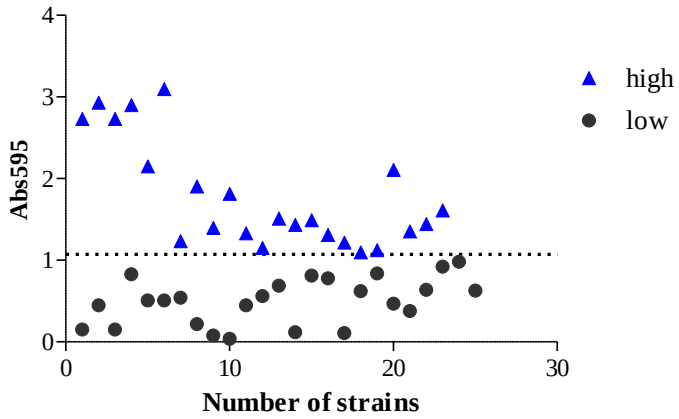

Figure 2. Distribution of 47 *P. aeruginosa* strains as biofilm formers. Low producer strains (black dots) and high producer strains (blue triangle). Each data point represents the mean of at least 3 replicates with SD removed for presentation. Broken line corresponds to PAO1 biofilm formation levels.

3. RELATIONSHIP BETWEEN VIRULENCE FACTORS LEVEL AND STAGE OF INFECTION IN THE 47 *P AERUGINOSA* CF ISOLATES

In order to investigate the dynamics of MvfR Quorum Sensing activity over pyocyanin producers *P. aeruginosa* strains, HHQ and PQS as well as the pro-persistent signal molecule 2-AA production at two time points (6 and 24 hours) using LC- MS/MS-based assay were performed. The results showed that less than 20% of the strains were able to produce higher levels of PQS, HHQ and 2-AA at 6 hours compared to the reference strain *P. aeruginosa* PA14; by contrast, at 24 hours, 68% of the strains were able to produce higher HHQ levels than PA14 and 52% of the strains secreted more 2-AA molecule than PA14. In general, most of the strains appeared to be low PQS producer compared to PA14; being only 25.5% of the strains able to produce PQS levels higher than those of *P. aeruginosa* PA14 at 24 hours (Figure 3).

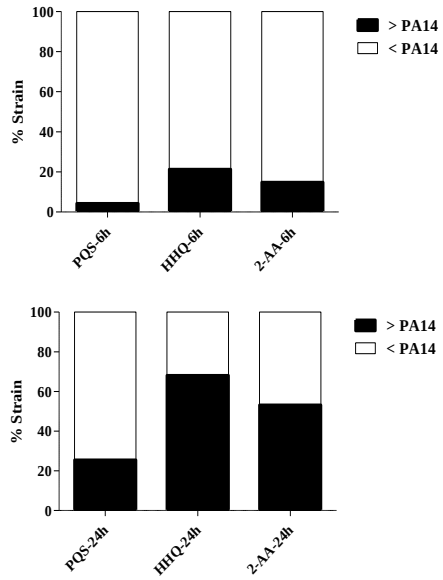

Figure 3. % *P. aeruginosa* isolates strains in function of PQS, HHQ and 2-AA production compared to basal levels of PA14 reference laboratory strain.

Levels of HAQs molecules and 2-AA molecules for each individual strain is shown in (Supplementary Information, Table 1S).

4. ANTIMICROBIAL SUSCEPTIBILITY PROFILES

Susceptibility profile of the 47 selected strains, using different class of antibiotics usually prescribed for the treatment of *P. aeruginosa*-driven infections (third generation cephalosporins, carbapenems, ß-lactam/ß-lactamase inhibitor combinations, aminoglycosides, fluoroquinolones and polymyxins) was determined by VITEK 2 apparatus.

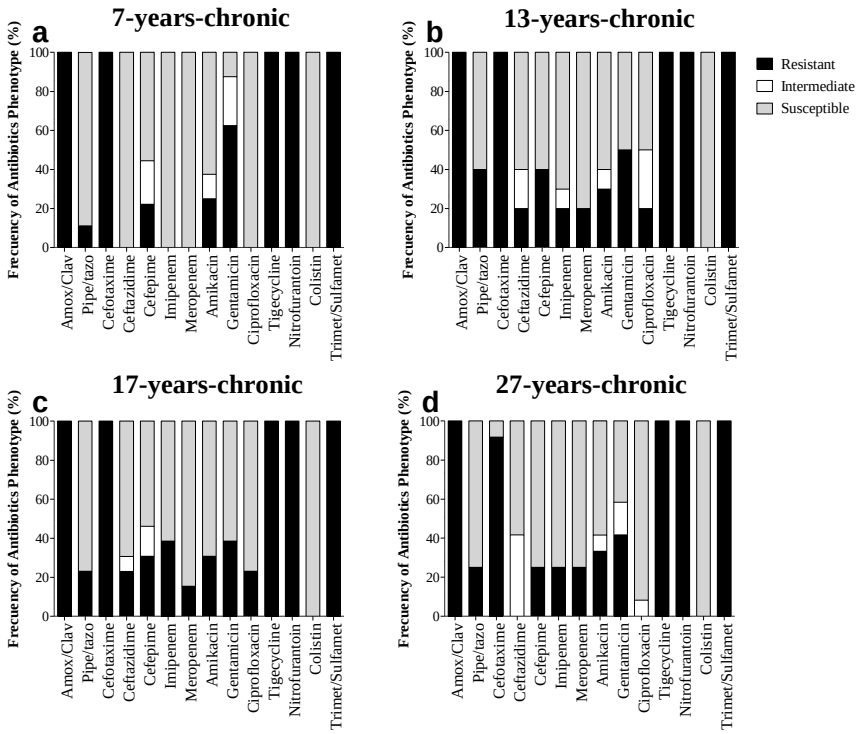

Figure 4. Antimicrobial susceptibility profile over chronicity time groups. a)Group-7-years-chronic, b)group-13-years-chronic, c)group-17-years-chronic and d) group-27-years-chronic..

The different antimicrobial susceptibility profile was analysed as function of the stage of infection (number of years). In the first instance, the 47 strains were clustered in four groups by stage of infection. For each group mean ± SD of years of infection was calculated: group-7-years-chronic (7.4 ± 2.2 years), group-13-years-chronic (13.5±1.4 years), group-17-years-chronic (17.3±0.9 years) and group-27-years-chronic (26.9±3.8 years).

All *P. aeruginosa* strain (4 groups), intrinsically resistance to Amoxicillin/Clavulanic, Trimethoprim/Sulfamethoxazole, Tigecycline, Nitrofurantoin and Cefotaxime, were susceptible to Colistin, whereas 40-60% of the strains exhibited Gentamicin resistance across the four groups. Interestingly, early chronic colonization strains (group 7-years-chronic) were all susceptible to Meropenem, Imipenem and Ceftazidime, while a range between 20-25 % of later chronic colonization isolates (average group 13, 17 and 27-years-chronic) showed resistance to these antibiotics. Furthermore, all early chronic strains were sensible to Ciprofloxacin, whereas in the groups classified as 13 and 17-years-chronic around a 20% of the strains showed resistance to the fluoroquinolone antibiotic (Figure 4).

Although chronicity time did not show antimicrobial resistance trends, it seems that a light Ceftazime, Imipenem and Meropenem resistance trends increases with the time of chronicity (Figure 4).

5. CORRELATION BETWEEN VIRULENCE FACTORS AND CLINCAL OUTCOMES

Substantial variability within chronic groups was found for Force Expiratory Volumen in 1 second (FEV1) value, pyocyanin 24 hours production, biofilm 24 hours production, HAQs molecules and the 2-AA molecule. No clear temporal trends were apparent when we compared the different levels of virulence factors between the several chronicity groups.

Forced expiratory volume in 1 second (FEV1) is an established marker of cystic fibrosis (CF) disease progression that is used to capture clinical course and evaluate therapeutic efficacy. In the present study, a slight statistical significant difference (Oneway ANOVA followed by Dunnett's post-test, $p< 0.05$) of FEV1 value between 7-years-chronic, strains compared to 27-years-chronic isolates was observed suggesting that FEV1 value declines at later infection stage (Figure).

Notwithstanding, when the whole panel (47 strains) between the different phenotypes and clinical features of patients was compared, several relationships between phenotypes traits become apparent.

Levels of 2-AA molecule and biofilm formation were modestly correlated (Spearman $r = 0.51$, $p = 0.0002$; $r =0.47$ $p = 0.0008$, respectively). In addition, weakly positive correlations were emerged between PQS levels and both FEV1 and 2-AA molecule values (Spearman $r= 0.41$, $p= 0.0049$; $r=0.40$ $p= 0.0049$) (Figure 6)

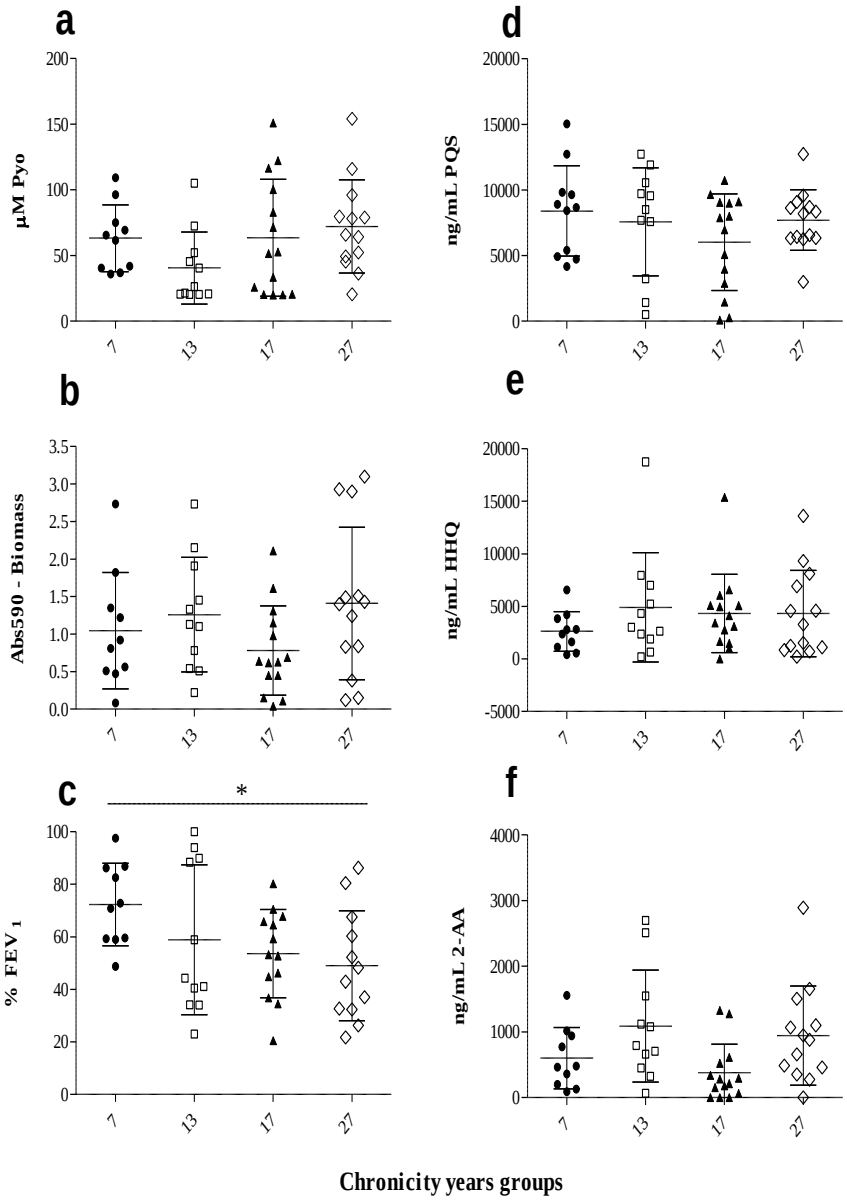

Figure 5. Distribution of different *P. aeruginosa* virulence factors and FEV_1 value in function of stage of infection. The 47 strains were divided in 4 groups in function of chronicity time until 2009. Mean ± SD of levels of a) pyocyanin, b) biofilm production, c) % FEV_1 value, d) PQS, e) HHQ and) 2-AA is reported for each group.

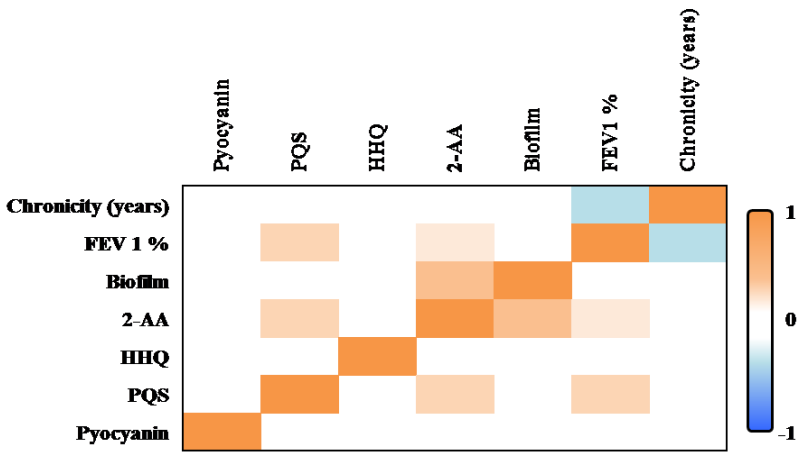

Figure 6. Correlation matrix of phenotype-phenotype and phenotype-features patients associations as determined by Spearman rank correlation coefficient. Orange indicates strong positive correlation between any given phenotype/feature pair (Spearman rank coefficient closer to 1) and while blue indicates strong inverse correlation (Spearman rank coefficient closer to -1) and white indicates no correlation between phenotype pairs (0).

6. SELECTION OF THE STRAIN FOR SET-UP AND VALIDATION OF CHRONIC LUNG INFECTION *IN VIVO* MODEL: *P. AERUGINOSA* ACC00901 STRAIN

P. aeruginosa ACC00901 was selected among the 47 panel isolates from cystic fibrosis patients in order to set-up a chronic lung infection in rat. This strain, isolated from the sputum of a CF patient 17 years after the onset of *P. aeruginosa* colonization, is characterized by a multi drug resistance (MDR) phenotype. This strain is a great biofilm and pyocyanin producer and, in addition to that, it produces levels of HHQ, PQS and 2-AA close to those of *P. aeruginosa* PA14. Normal exponential growth was observed in the strain when the growth ability was tested in LB medium up to 24h of incubation (Figure 7).

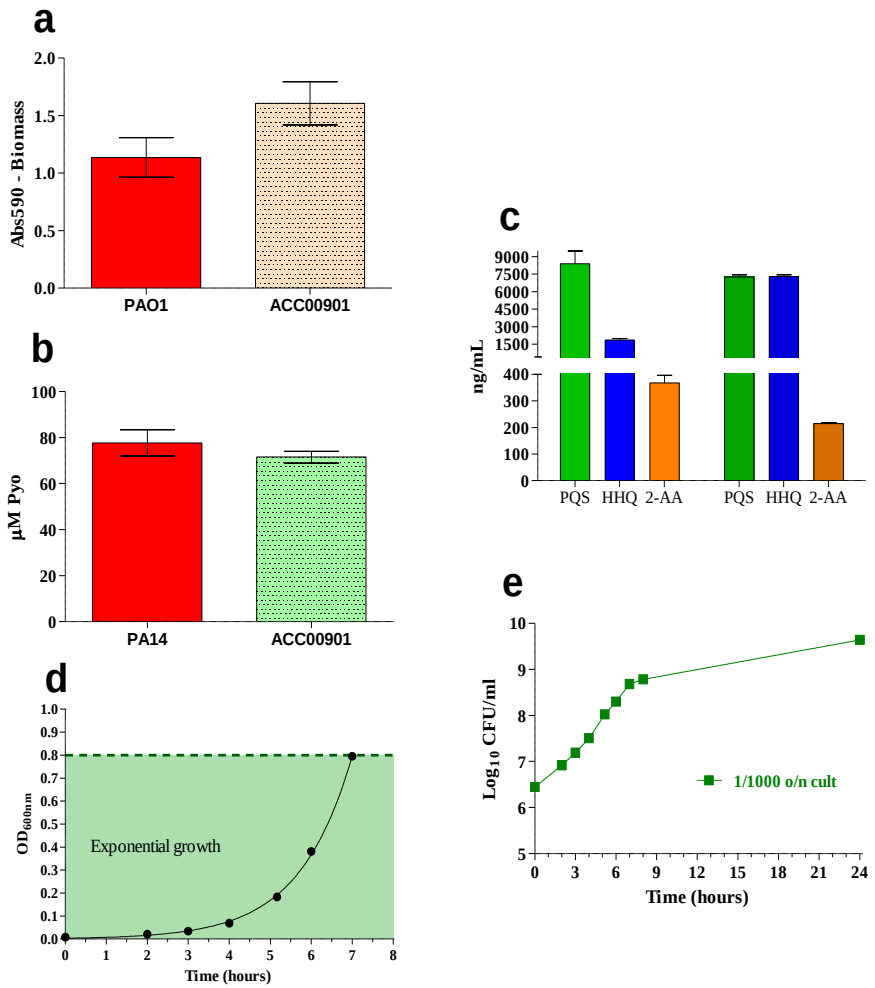

Figure 7. Full characterization of *P. aeruginosa* ACC00901. Biofilm formation (a), pyocyanin levels (b), HAQs molecules and 2-AA levels (c), growth curve OD_{600} (d) Growth curve Log CFU/mL(e) are reported.

DISCUSSION

Pseudomonas aeruginosa is a Gram-negative bacterium that causes opportunistic infections including burn wound infections, urinary tract infections, keratitis, otitis externa and respiratory tract infections in susceptible individuals. Chronic airway infections caused by *Pseudomonas aeruginosa* are the major cause of morbidity and mortality in cystic fibrosis patients as infections of this opportunist pathogen contribute to decline in lung function [2]–[5].

Most of the research performed and the validation of NCEs on *P. aeruginosa* has been focused on reference strains such as PAO1 or PA14, which has been showed to differ genotypically and phenotypically from the most abundant CF clinical isolates [6]. The potency of the compounds may vary in a strain dependent manner, thus from a drug discovery point of view, it is important to include multiple strains to validate NCEs in a screening cascade. Even if there is a considerable body of literature studying several panel strains of CF clinical isolates [7]–[9], the analysis were mainly focused on the characterization of general trends of CF chronic isolates, such as mucoid and non-mucoid phenotypes, colonies morphology, biofilm formation or antimicrobial susceptibility. Nowadays, it is present a shortage of a CF panel strains characterized in function of MvfR virulence factors. Based on these needed, here we report a specific MvfR QS phenotypic characterization, including pyocyanin, PQS, HHQ, and 2-AA molecules across a panel of clinical strains isolated from sputum of chronic cystic fibrosis patient at different stage of infection. Biofilm formation and antimicrobial susceptibility was also assessed. Finally, a relation between the different phenotypes, stage of infection and clinical outcomes, were attempted.

Pyocyanin is a terminal signal factor in the MvfR QS of *P. aeruginosa* and it acts as a major virulence factor of this opportunistic pathogen [10]. Its

production was variable across the 109 panel strain reported in this study. 47.92% (n=47) of the strains showed *in vitro* pyocyanin production over 20 µM. Over this bacterial panel, 80% of the clinical isolates were lower HAQs molecules producer at 6 hours than PA14 reference strain. However at 24 hours, 68% of the CF strains were able to produce higher HAQs molecules than PA14 strain, in particularly, HHQ levels. Actually, most of the HAQs signal molecule, in particularly PQS, are produced at the end of the exponential phase [11]. The production of HAQs molecules at 6 hours could be explained as CF clinical isolate strains are characterized by slow growth, so it takes more time to achieve the end of the exponential phase, delaying in this way the start point of HAQs molecules synthesis. In general, most of the panel strain seems to be low PQS producer compared to PA14 at 24 hours; actually only a 25.5% of the CF panel strain was able to produce higher PQS levels than *P. aeruginosa* PA14. This might be attributed to the high frequency of *las* mutant in CF chronic strains. HHQ is converted into PQS by the action of PqsH, a putative flavin-dependent monooxygenase and it has been demonstrated that the transcription of pqsH is controlled by LasR, implying that the PQS system is controlled by the las system[12]. Diggle *et al.* have analysed spent *P. aeruginosa* culture supernatants revealing that PQS is produced at the end of exponential phase in the parent strain and in the late stationary phase of a *las* mutant [11].

Cullen *et al* carried out the phenotypic characterization of a panel of CF strains suggesting a trade-off between strong biofilm formation and low pyocyanin production [13]. However, in the present study our pyocyanin producer panel of *P. aeruginosa* were uniform distributed between low (51.06% of the strains) and high (48.94% of the strains) biofilm formation levels. Moreover, no Spearman correlation was found between these two phenotypes. On the other hand, a moderately relation between biofilm formation and the production of the small volatile molecule 2-AA (Spearman

correlation r = 0.51, $p< 0.0002$) was positively correlated. It has been demonstrated that this small volatile molecule, synthesized by *pqsABCD* operon enzymes which are under transcriptional control of the MvfR [14], promotes the emergence of persistent *P. aeruginosa* strains that likely promote chronic lung infections behaviours [15], such as biofilm formation [16]. That could be an explanation of why high levels of 2-AA has been related with high biofilm production in our studies, since all the isolates belong to *P. aeruginosa* chronic CF patients. In any case, further studies should be performed to confirm this interesting connection.

The panel comprised 47 strains were classified in four groups in function of stage of infection (years of chronicity): group-7-years-chronic (7.4 ± 2.2 years), group-13-years-chronic (13.5 ± 1.4 years), group-17-years-chronic (17.3 ± 0.9 years) and group-27-years-chronic (26.9 ± 3.8 years) in order to attempt relations between the stage of infection and the MvfR phenotypes evaluated on the present study. No clear temporal trends were evident when we compared the different levels of virulence factors and biofilm formation between the different stages of infection. A high variability within and between groups was observed. Only a slight statistical significant difference of % FEV_1 value between 7-years-chronic strains compared to 27-years-chronic isolates was observed suggesting FEV_1 value declines at later infection stage. Thus, *in vitro* MvfR phenotype across the CF panel strain selected for this study could not distinguish between early and later chronic infection stages.

On the other hand, the full characterization of 47 strains, allowed us identifying *P. aeruginosa* ACC00901, which has an MDR phenotype and is a great biofilm and pyocyanin producer. Additionally, it produces levels of HHQ, PQS and 2-AA close to those of *P. aeruginosa* PA14. For these reasons *P. aeruginosa* ACC00901 strains is a suitable candidate for the set-up of a chronic lung infection.

SUPPLEMENTARY INFORMATION

Table 1S. Clinical outcomes of patients from whom *P. aeruginosa* clinical strains were isolated. All the data belongs to the CF Collection Database of Azienda Ospedaliera Universitaria Integrata di Verona (Centro Regionale Fibrosi Cistica)

CF Strain	Mean FEV1 in 2009	First data of *P. aeruginosa* isolation	Time of chronicity until 2009
788	92.5	26-Apr-89	20
789	80.5	16-Nov-92	17
790	26.4	02-May-02	7
791	72.75	30-Nov-00	9
792	34.5	23-Jul-91	18
793	46.25	28-May-91	18
794	91.72	20-Feb-90	19
795	67.55	12-Jul-79	30
796	35.5	06-Sep-01	8
797	31.23	11-Feb-93	16
798	39.53	27-May-91	18
799	96.33	31-May-91	18
800	36.87	18-Mar-96	13
801	101	07-Jun-88	21
802	60.33	22-Jul-82	27
803	72.5	12-Mar-98	11
804	44.3	01-Aug-95	14
805	53	15-Dec-82	27
806	42.99	29-Jan-82	27
807	44.12	22-Feb-02	7
808	70.75	18-Nov-03	6
809	27.5	23-Sep-91	18
810	30.45	07-Oct-77	32
811	31.73	11-Jan-93	16
812	51.2	29-Nov-05	4
813	53.2	06-Sep-95	14
814	48.9	30-Aug-91	18
815	48.2	28-Apr-95	14
816	27.6	13-Dec-93	16

CF Strain	Mean FEV1 in 2009	First data of *P. aeruginosa* isolation	Time of chronicity until 2009
817	23.42	16-Sep-91	18
818	24.1	24-May-91	18
819	59	22-Jul-91	18
820	33.11	08-Apr-01	8
821	62.75	17-Feb-97	12
822	34.09	09-May-97	12
823	30.73	02-Feb-80	29
824	40.5	14-May-95	14
825	106.5	02-May-95	14
826	35.81	31-Aug-99	10
827	41	02-Jun-86	23
828	41	21-May-04	5
829	25.5	20-Feb-92	17
830	23	12-Oct-95	14
831	56.7	02-Apr-92	17
832	21.69	13-Jun-76	33
833	59	02-Jan-00	9
834	36.88	21-Mar-91	18
835	48.75	13-Jul-07	2
836	33.53	01-Jan-92	17
837	35	06-May-91	18
838	49.8	09-Jan-86	23
839	35.08	16-Jul-91	18
840	39.62	17-Dec-07	2
841	20.5	25-Jun-91	18
842	33.8	26-May-91	18
843	86.25	29-Dec-03	6
844	59.28	12-Jul-91	18
845	88.46	25-Jan-96	13
846	32.72	28-May-80	29
847	80.25	14-Feb-90	19
848	68.85	11-Nov-85	24
849	63.16	10-Dec-87	22
850	57.6	12-Oct-78	31

CF Strain	Mean FEV1 in 2009	First data of *P. aeruginosa* isolation	Time of chronicity until 2009
851	86.75	27-Nov-96	13
852	53.75	05-Aug-91	18
853	32.36	11-Jul-77	32
854	37.07	03-Apr-82	27
855	42.88	29-Sep-87	22
856	76.23	06-Dec-99	10
857	68.25	26-Jul-92	17
858	86.25	18-Aug-88	21
859	65.9	12-Aug-91	18
860	82.5	31-Oct-00	9
861	58.88	28-Oct-98	11
862	37.5	06-Jun-96	13
863	59.54	30-Apr-01	8
864	67.88	23-Jun-92	17
865	59.66	28-Jan-02	7
866	49.5	27-Mar-01	8
867	44.85	20-Jun-91	18
868	34	17-Feb-97	12
869	80.43	19-Jan-85	24
870	47.41	24-Jul-07	2
871	86.8	08-Jul-99	10
872	56.87	14-Jun-88	21
873	28.92	08-Mar-82	27
874	41.09	08-Mar-95	14
875	26.3	28-Jan-85	24
876	53.33	13-Aug-92	17
877	64.57	09-Sep-91	18
878	59.25	19-Jan-01	8
879	52.75	01-Nov-92	17
880	83.9	27-Aug-87	22
881	68	17-Oct-80	29
882	52.25	10-Sep-77	32
883	70.5	02-Jul-91	18
884	28.23	16-Sep-91	18

CF Strain	Mean FEV1 in 2009	First data of *P. aeruginosa* isolation	Time of chronicity until 2009
885	55.16	27-Jul-94	15
886	36.5	08-Jan-92	17
887	71.66	16-Jul-91	18
888	93.57	06-Oct-94	15
889	45.15	21-Oct-84	25
890	63.5	23-Oct-91	18
891	23.45	10-Sep-96	13
892	94.04	09-Aug-94	15
893	97.66	06-Mar-01	8
894	48.31	19-Aug-86	23
895	89.95	15-Jul-93	16
896	89.83	31-Aug-01	8
901	35.6	15-Jan-1992	17

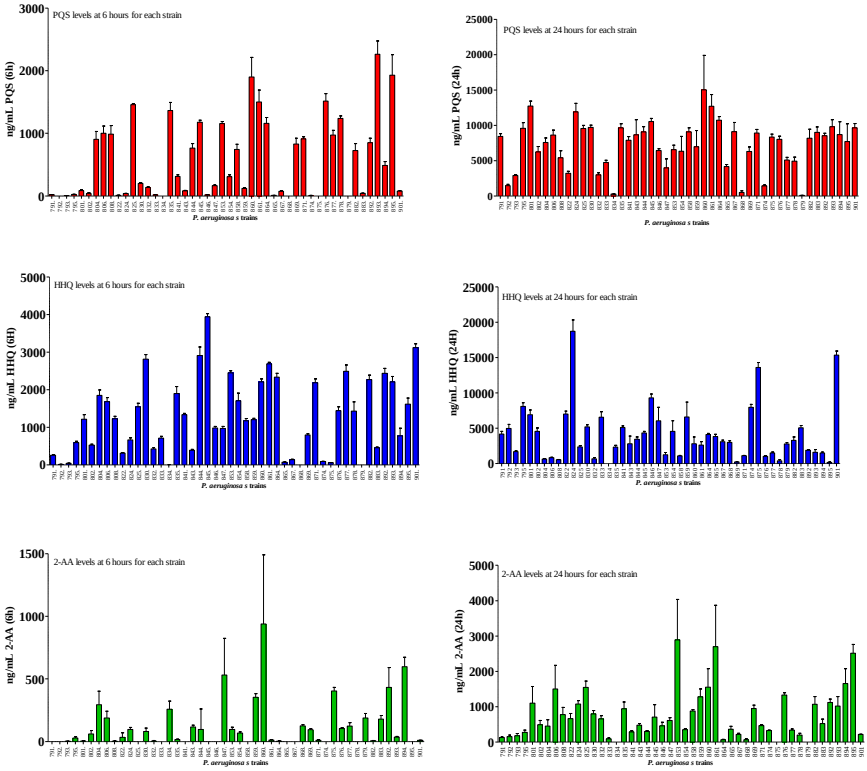

Figure S 1.Basal levels (ng/mL) of PQS (red bars), HHQ (blue bars) AND 2-AA (green bars) at both 6h and 24h for each individually strain. Bars represent the mean of at least 3 replicates. Error bars show the SD for each sample.

REFERENCES

[1] O. Albarbarawi, G. Devereux, and J. T. Huang, 'Characterization and validation of an isotope-dilution LC – MS / MS method for quantification of total desmosine and isodesmosine in plasma and serum', pp. 1991–2001, 1991.

[2] K. Cheng *et al.*, 'Spread of beta-lactam-resistant *Pseudomonas aeruginosa* in a cystic fibrosis clinic', *Lancet*, 1996.

[3] F. W. Scott and T. L. Pitt, 'Identification and characterization of transmissible Pseudomonas aeruginosa strains in cystic fibrosis patients in England and Wales', *J. Med. Microbiol.*, 2004.

[4] M. L. Workentine *et al.*, 'Phenotypic Heterogeneity of Pseudomonas aeruginosa Populations in a Cystic Fibrosis Patient', *PLoS One*, 2013.

[5] C. Winstanley, S. O'Brien, and M. A. Brockhurst, 'Pseudomonas aeruginosa Evolutionary Adaptation and Diversification in Cystic Fibrosis Chronic Lung Infections', *Trends in Microbiology*. 2016.

[6] J. Klockgether *et al.*, 'Genome diversity of Pseudomonas aeruginosa PAO1 laboratory strains', *J. Bacteriol.*, 2010.

[7] N. Høiby, O. Ciofu, and T. Bjarnsholt, 'Pseudomonas aeruginosa biofilms in cystic fibrosis', *Future Microbiology*. 2010.

[8] P. Owlia, R. Nosrati, R. Alaghehbandan, and A. R. Lari, 'Antimicrobial susceptibility differences among mucoid and non-mucoid Pseudomonas aeruginosa isolates.', *GMS Hyg. Infect. Control*, 2014.

[9] S. T. Clark *et al.*, 'Phenotypic diversity within a Pseudomonas aeruginosa population infecting an adult with cystic fibrosis', *Sci. Rep.*, vol. 5, no. June, pp. 1–10, 2015.

[10] L. E. P. Dietrich, A. Price-Whelan, A. Petersen, M. Whiteley, and D. K. Newman, 'The phenazine pyocyanin is a terminal signalling factor in the quorum sensing network of Pseudomonas aeruginosa', *Mol. Microbiol.*, 2006.

[11] S. P. Diggle, K. Winzer, S. R. Chhabra, K. E. Worrall, M. Cámara, and P. Williams, 'The Pseudomonas aeruginosa quinolone signal molecule overcomes the cell density-dependency of the quorum sensing hierarchy, regulates rhl-dependent genes at the onset of

stationary phase and can be produced in the absence of LasR', *Mol. Microbiol.*, 2003.

[12] J. W. Schertzer, M. L. Boulette, and M. Whiteley, 'More than a signal: non-signaling properties of quorum sensing molecules', *Trends Microbiol.*, vol. 17, no. 5, pp. 189–195, 2009.

[13] L. Cullen *et al.*, 'Phenotypic characterization of an international pseudomonas aeruginosa reference panel: Strains of cystic fibrosis (cf) origin show less in vivo virulence than non-cf strains', *Microbiol. (United Kingdom)*, vol. 161, no. 10, pp. 1961–1977, 2015.

[14] G. Xiao, J. He, and L. G. Rahme, 'Mutation analysis of the Pseudomonas aeruginosa mvfR and pqsABCDE gene promoters demonstrates complex quorum-sensing circuitry', *Microbiology*, vol. 152, no. 6, pp. 1679–1686, 2006.

[15] M. Kesarwani *et al.*, 'A quorum sensing regulated small volatile molecule reduces acute virulence and promotes chronic infection phenotypes', *PLoS Pathog.*, 2011.

[16] N. Q. Balaban, J. Merrin, R. Chait, L. Kowalik, and S. Leibler, 'Bacterial persistence as a phenotypic switch', *Science (80-.).*, 2004.

Chapter 4

Mild Lung Infection Model induced by intratracheal administration of *P. aeruginosa* ACC00901-agar beads

EXECUTIVE SUMMARY

In this section, design, set-up and validation of a rat model of chronic lung infection required for understanding the pathogenesis of lung diseases, such as, cystic fibrosis with infecting bacteria and to evaluate new compounds and/or different therapeutic approaches is reported. The main challenge for the development of the model was to find a suitable bacterial strain able to induce a sustained chronic infection, without any clearance from the host.

The approach pursued was to explore the model of chronic lung infection with two strains, namely *P. aeruginosa* Xen41, a bioluminescence isogenic strain of *P. aeruginosa* PAO1 strain, and *P. aeruginosa* ACC00901, a clinical strain isolated from the sputum of a CF-patient.

A specific procedure for incorporation of the strains into agar beads was developed. Agar beads containing *P. aeruginosa* Xen41 or *P. aeruginosa* ACC009001 were *in vitro* prepared and infection induced by intratracheal administration in CD male rats. Evaluation of Body Weight (BW) and Clinical Score (CS), Colony Forming Unit (CFU)in lungs, and histology (lungs) were assessed. The chronic lung infection model, carried out with *P. aeruginosa* ACC00901 was validated with Tobramycin.

MATERIALS AND METHODS

1. BACTERIAL STRAINS

P. aeruginosa Xen41 strain derived from parental strain PAO1, is a bioluminescence (BLS) bacteria for *in vivo* and *in vitro* drug discovery. It possesses a stable copy of the Photorhabdus luminescens *lux* operon on the bacterial chromosome. In the present study, *P.aeruginosa*. Xen41 was used for the set-up of mild lung infection model. That pathogen allowed the evaluation of infection (up to day 15) using *ex vivo* BLS (IVIS image®).

P. aeruginosa ACC00901 strain was isolated from sputum of CF patient at a late point in time during chronic lung infection. The pathogen was selected from the previous phenotype characterization of 47 CF-chronic strains.

2. ANIMALS

All the animal studies were conducted in accordance with national legislation and under authorization issued by the Italian Ministry of Health (**Project Code No. 21201**). Aptuit is committed to the highest standards of animal welfare and is subject to legislation under the Italian Legislative Decree no. 26/2014.

Both for chronic lung infection set-up and for the validation method with Tobramycin, rats CD male (Charles River, Italy) weighing between 200-225 grams at the start of the experiment were housed in groups in solid bottom plastic cages (Eurostandard Type IV 595x380x200mm) with sawdust litter/enrichment material during 5 days as minimum acclimatisation. Food (A. Rieper SpA, Bolzano, Italy) and water (filtered from normal domestic supply) were available ad libitum. Fluorescent lighting where switch on approximately from 6 to 18 hours daily.

3. INOCULUM PREPARATION

Agar beads including *P. aeruginosa* Xen41 and ACC00901 were performed according to the procedure describe *by* Kukavica-Ibrulj *et al.* with little modifications. [1]. Briefly, an overnight culture both of *P. aeruginosa* Xen41 and *P. aeruginosa* ACC00901 was prepared in LB broth and sub-cultured in LB fresh medium until the absorbance at 600 nm reached a value in the range of 0.6-0.8 OD. Exponential cultures were then collected, centrifuged and re-suspended in PBS. Bacteria was embedded into agar beads by mixing the culture with molten 2% w/v agar in PBS which was then spun into warmed mineral oil. Mineral oil was cooled, beads centrifuged and then washed with PBS pH 7.2 containing 0.5% (w/v) SDC and PBS pH 7.2 containing 0.25% (w/v) SDC. Agar beads were then centrifuged and washed three times with PBS and CFU/mL determined and BLS was measured for Agar-Beads containing *P.aeruginosa*. Xen41 strain. Sterile beads to treat control group (blank agar beads) were prepared in the same way without including bacteria. To determine CFU, bacteria enmeshed in beads are released using a Polytron. The Polytron probe is sterilized by immersing the probe in a 50 mL tube containing 10 mL of ethanol 70 % and rinsed in a tube containing 10 mL of sterile water. Homogenize 1.5 mL of the bead slurry + 1.5 mL PBS (1:2 dilution) in a 15 mL Falcon tube with the Polytron using a burst of 3x10s. Prepare serial dilution (up to 10^{-6}) of the homogenized bead slurry and plate on LB agar plates. Incubation of plates was carried out at 35°C ±2 overnight. This procedure was used for both set-up infection and validation experiments.

4. ANTIBIOTIC AND DOSAGE REGIMEN

Tobramycin (BEW= 1.427) antibiotic was purchased by Sigma-Aldrich (Italy).

Tobramycin Sulphate solutions were freshly prepared in water and stored at 4°C prior to use. Two different regimen of dosage were used, 0.5mg/die and 1mg/die. The therapy was intratracheal daily administrated during 4 days (from day 3 to day 7 post-infection) (Figure 2).

5. INFECTION ANIMAL PROCEDURE – SET-UP CHRONIC INFECTION MODEL

On the day of infection, 33 isoflurane-anesthetized CD male rats/strain/experiment (n_{total}=66) were intratracheal inoculated with a suitable device with blank agar beads, or including the selected strain Xen41 and ACC00901 (inoculum size ~6Log CFU/rat) and allocated to the different groups in function of time points sacrifice (time point, 2,7,10 and 15 day post-infection). For each time point, 4 infected animals and 3 non infective (controls blank Agar Beads) were sacrificed for evaluation of CFU in lungs. and BLS in lung (BLS only in *P. aeruginosa* Xen41). Body Weight (BW), Survival rate (SR) and clinical score were assessed at 0,1,2,3,6,7,8,9,10 and 15 day post-infection. (Figure 1).Two more ACC00901 infected rats were used at day 7, 10 and 15 for lung histology.

At the end of the experiment, overdose of inhaled 5% isoflurane followed by bleeding from the abdominal aorta was performed as method of euthanasia.

The statistical significance difference in bacterial count (CFU/day) between different time point of infection (compared to T0, initial infection) was calculated using the one-factor ANOVA followed by Dunnett's test ($p<0.05$).

6. VALIDATION OF *IN VIVO* MODEL - TOBRAMYCIN

On the day of infection, 35 isoflurane-anesthetized CD male rats/strain/experiment (ntotal= 36) were intratracheally inoculated with a suitable device with blank agar beads (n=7) or including the *P. aeruginosa*. ACC00901 strain (n=28) (inoculum ~ 6.0 Log CFU/rat).

In order to verify stage of infection before starting treatment, 7 rats were sacrificed at day 3 post-infection for measuring CFU in lung. Then, a total of 21 rats (7 animals/treatment) were treated intratracheally with saline solution, with 0.5mg/die and 1.0 mg/die of Tobramycin.

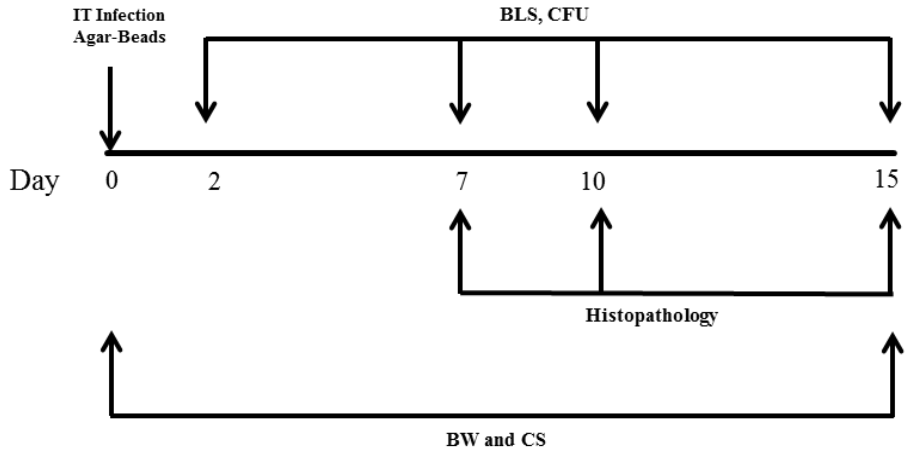

Figure 2.Experimental design of chronic lung infection set-up.

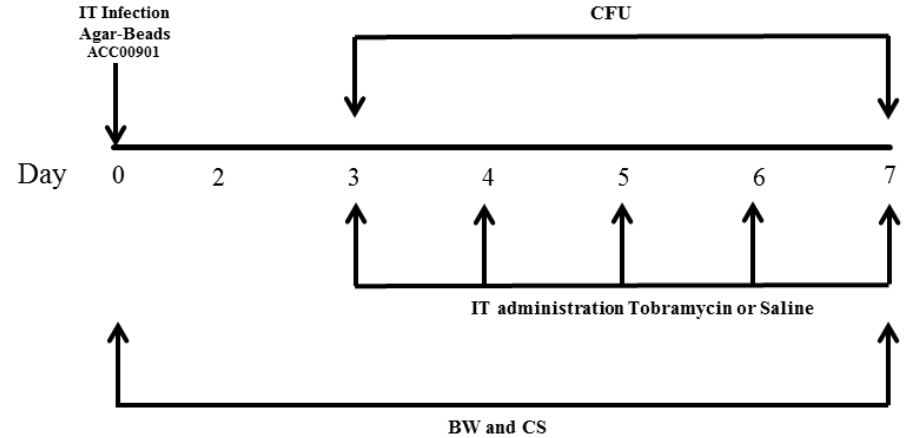

Figure 1. Experimental design of chronic lung infection validation with Tobramycin.

In order to monitor the treatment, Body Weight (BW) and Clinical Score (CS) were recorded during 7 days of infection. Moreover, CFU of lungs were measured at the end of the treatment over 7 animals/treatment (day 7 post-infection) (Figure 2).
The statistical significance difference in bacterial count between control and treated rats was calculated using the one-factor ANOVA followed by Dunnett's Test ($p<0.05$).

RESULTS

1. AGAR-BEADS PREPARATION

P. aeruginosa agar beads were successfully prepared. Distribution size of the agar beads, containing bacteria was enough homogenous (~100 μm). The three measures of particle size were high reproducible, indicating a homogenous distribution of agar beads on sample preparation (Figure 3). Agar beads stability conserved at 4^0C was assessed counting CFU at day 5, 8 and 20 post-preparation. Great stability over time was confirmed (~ 7.5 Log CFU/mL/ time point).

2. SET-UP OF MILD CHRONIC LUNG INFECTION IN RAT

Body weight and clinical score during 15 days of infection

Body weight (BW) and clinical score (CS) highlight that *P. aeruginosa* Xen41 agar beads infected animals show to be "*on crisis*" during the first 2 days post infection (loss of BW and increment of CS) (Figure 4) whereas rats infected with *P. aeruginosa* ACC00901 agar beads, showed very low signs of discomfort within two days from infection (poor BW loss and small increment of CS) (Figure 4).

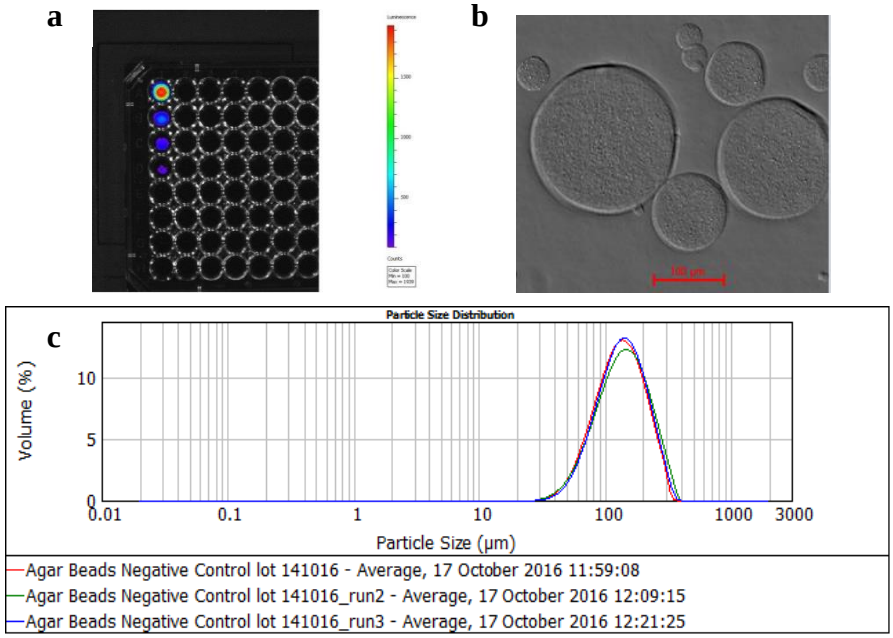

Figure 3. *P. aeruginosa* Xen41 embedded in agar beads. a) Bioluminescence evaluation at different dilutions (from 10^{-8} to 10^{-4}). b) Microscope image of the agar beads containing the pathogen. c) Distribution agar beads size over sample.

Bacterial count in lungs during infection

A sustainable localized chronic infection is detected during 15 days. On average, 5.6 Log CFU/g of tissue are still present in lungs at day 15 (both strains) (Figure 5). On the other hand, mortality observed within the first 2 days of infection, is about 30% for *P. aeruginosa* Xen41 and a 0% for *P. aeruginosa* ACC00901 (Figure 5).

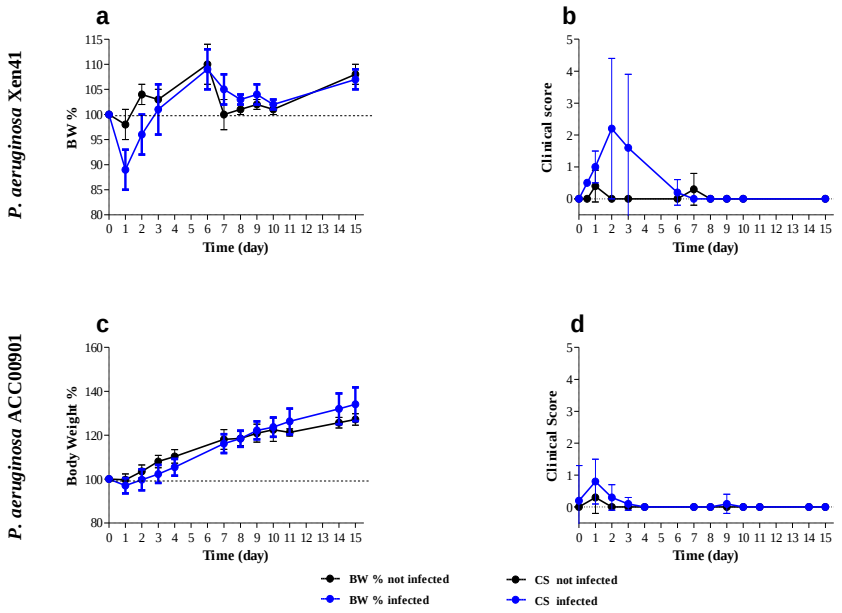

Figure 4.a) Body weight and **b)** Clinical score trend of animals infected with *P. aeruginosa* Xen41 recorded during 15 days of infection. **c)** Body weight and **d)** Clinical score trend of animals infected with *P. aeruginosa* ACC00901 recorded during 15 days of infection

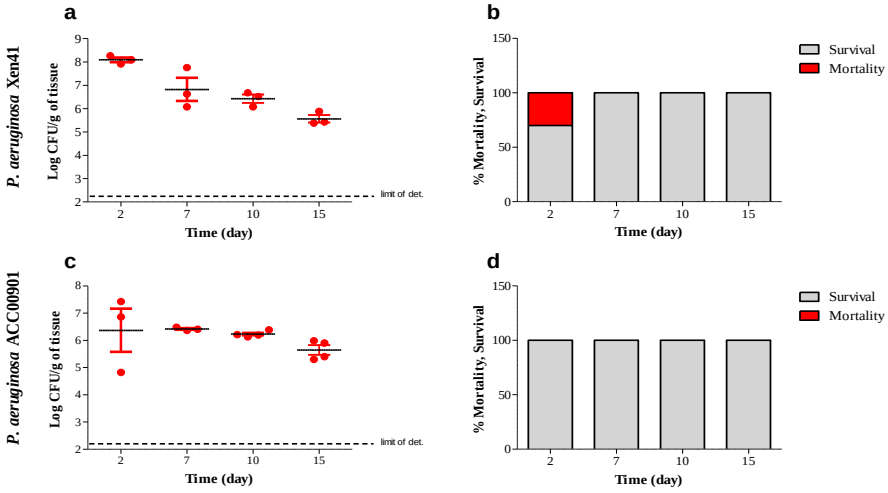

Figure 5. Time course of *P. aeruginosa* chronic infection with Xen41 and ACC00901 strains. Animals were infected by intratracheal injection of *P. aeruginosa* Xen41 or *P. aeruginosa* ACC00901 agar-beads. Growth curves of Xen41 (a) and ACC00901(c) strains in rats lungs are showed (Dots represent individual measurements and horizontal lines represent mean values). Histograms (**b** and **d**) represent the percentage mortality present during time course infection.

Ex vivo lung bioluminescence and macroscopic examination

Macroscopic examination and *ex vivo* BLS confirmed the presence of an acute infection at day 2 that evolved in chronic up to day 15. The weight of lungs of infected animals highlights a hypertrophic status due to the huge presence of infiltrates at day 2 (Figure 8)

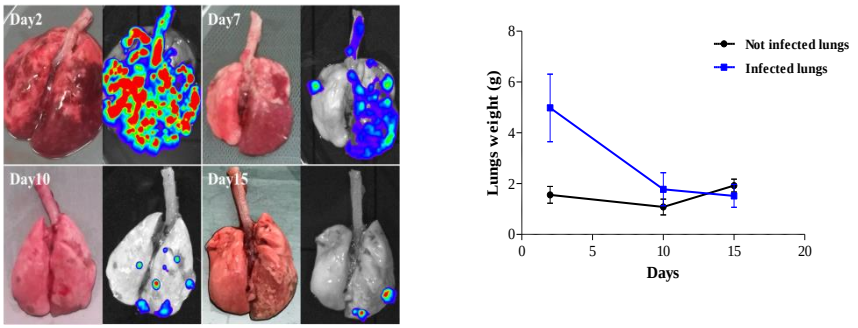

Figure 6.a) Bioluminescence evaluated using IVIS image® and macroscopic examination lungs during chronic infection with *P. aeruginosa* Xen41. b) Weight of lungs over the infection time of *P. aeruginosa* Xen41

Histopathology of lungs

Histopathology results showed how at the beginning the bacteria remaining in agar beads, grew in communities and produced biofilm to avoid the pro inflammatory response (day 7). At day 10 of infection, bronchus was filled by a massive neutrophil inflammation around the agar bead. At the end of the infection (day 15) the histopathology lung showed neutrophils infiltrating the parenchyma while ACC00901 bacteria left the agar beads and established the chronic infection (Figure 9).

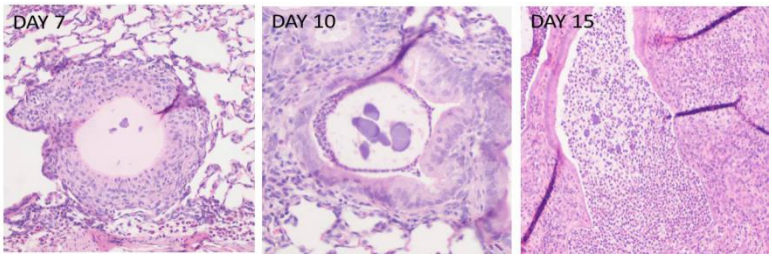

Figure 7.Histological sections of lungs after 7,10 and 15 days of chronic infection with ACC009001 clinical strain.

3. VALIDATION OF CHRONIC LUNG INFECTION

Body weight and clinical score during 7 days of infection

Body weight (BW) and clinical score (CS) highlighted that rats infected with *P. aeruginosa* ACC00901 agar beads showed low signs of discomfort within two days from infection (loss of BW < 20% and slight increment of CS).Then, all recorded parameters recovered a physiologic trend in the following days.

Bacterial count in lungs during infection

At 3 day post infection, before start of therapy, 7.8 Log CFU/g tissue of lung average were present. Rats treated with both saline (vehicle) and Tobramycin at regimen of dosage 0.5 and 1 mg/die showed a significant reduction of respectively 1.04 and 1.31 Log CFU/g tissue of lung with respect to animals treated with saline (Figure 11).

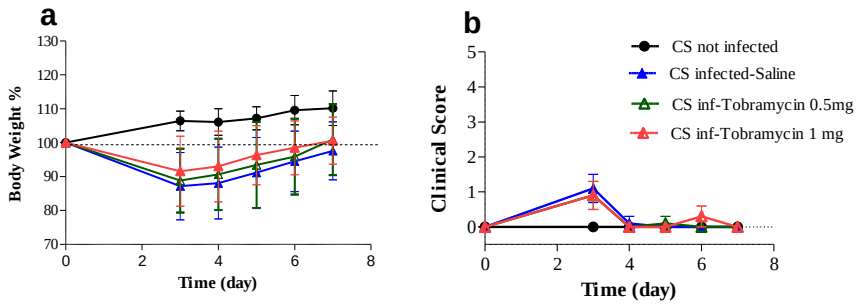

Figure 9.a) Body weight and **b)** clinical score recorded of animals infected with *P. aeruginosa* ACC00901 treated with saline (blue), treated with 0.5mg/day of Tobramycin (green), treated with 1mg/day (red) and not infected animals (black) up to 7 days.

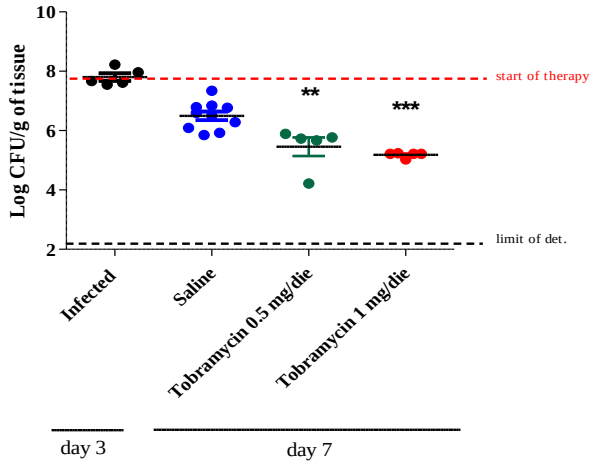

Figure 8.Bacterial counts (Log CFU/ml) in lungs at the start/end of therapy with Tobramycin or saline. Animals infected with *P. aeruginosa* ACC00901 treated with both saline (blue) and Tobramycin 0.5 mg/day (green) or 1 mg/day (red) were recorded at day 7 (end of the therapy). Data are expressed as scatterplot distribution included mean. Statistical analysis was performed by a Oneway ANOVA followed by Dunnett'sTest (groups vs day 3(start of therapy), *p<0.05).

DISCUSSION

Development of a chronic lung infection animal model is top priority for the assessment of novel therapies useful to treat CF infections.

Until now, several studies showed acute-pneumonia model useful to study both non-CF related pneumonia and initial phase of lung infection during *P. aeruginosa* colonization of CF airway [2][3]. The aerosol instillation or directly intratracheal administration of a saline bacteria suspension provides rapid clearance of the organism or acute sepsis and death. The development of chronic lung infections needs to overcome the lethal score and the rapid clearance occurring at early stage of the infection. In 1979, Cash *et al* [4] established the first animal model of chronic *P. aeruginosa* lung infection in rats, suggesting that the long-term infection can be achieved by inoculating bacteria embedded in agar beads as an immobilizing agent. As time goes by, several animal models using immobilizing agents for chronic infection have been described [5] [6].

In the present study, we have explored the differences between infection with an isogenic PAO1 bioluminescence strains (*P. aeruginosa* Xen41) and a *P. aeruginosa* clinical strains isolated from the sputum of a 17-years-chronic Cystic Fibrosis patients (ACC00901), both of them embedded in agar beads. The results until now showed the importance of type of bacteria loading into agar beads. Both *P. aeruginosa* Xen41 and ACC00901 were able to induce a 15-day chronic lung infection. Number of bacteria at day 2 post infection was higher for Xen41 (8.09 ± 0.17 Log CFU/lung) compared to AC00901 (6.37 ± 1.37 Log CFU/lung). Anyway, when chronic infection was stablished the bacteria burden was uniform for both strains with 5.6±0.3 Log CFU/lung on average. However, mortality at first days of infection was higher in rats infected by the bioluminescence *P. aeruginosa* Xen41 (30% of mortality) than *P. aeruginosa* ACC00901 (100% survival). Based on that, rats infected

with Xen41 strains presented loss of weight body and an increment on clinical score within the 2 days-post infection while, *P. aeruginosa* ACC00901 showed less signals of discomfort.

The initial histopathology carried out over ACC00901 lung infected allowed us to observe agar beads in bronchial lumen at day 7 containing burden bacteria. As Faccini *et al*. observed [7], the bacteria grew in form of microcolonies under the microaerobic/anaerobic environments of the agar bead, mimic the grow in the mucus of Cystic Fibrosis patients[6]. At day 15 post infection, the histopathology sample showed neutrophils infiltrating the parenchyma while ACC00901 bacteria left the agar beads and established the chronic infection.

Even if *P. aeruginosa* ACC00901 showed *in vitro* high levels of HAQs molecules (*Chapter 3*), *in vivo* levels of those were almost imperceptible on lung homogenate at day 7 post-infection (data no shown). Only low levels of HHQ were present on the sample. The read out of quorum sensing molecules in *in vivo* models need further exploration.

Validation of *P. aeruginosa* ACC00901 lung infection model was carried out with Tobramycin (MIC = 0.5 μg/mL). At day 3 post infection, 7.8 Log CFU/g tissue of lung on average were present before the start of therapy. Rats treated with Tobramycin at regimen of dosage 0.5 and 1 mg/die showed a significantly reduction of respectively 1.04 and 1.31 Log CFU/g with respect to animals treated with saline.

In summary, Chronic lung infection rat model induced by intra-tracheal administration of agar beads containing *P. aeruginosa ACC00901 (*preferable than isogenic PAO1 strain) was set –up and validated with Tobramycin.

REFERENCES

[1] A. Filloux and J. M. Walker, *Pseudomonas IN Series Editor*. 2014.

[2] M. Allewelt *et al.*, "Acquisition of Expression of the Pseudomonas aeruginosa ExoU Cytotoxin Leads to Increased Bacterial Virulence in a Murine Model of Acute Pneumonia and Systemic Spread Acquisition of Expression of the Pseudomonas aeruginosa ExoU Cytotoxin Leads to Increase," vol. 68, no. 7, pp. 3998–4004, 2000.

[3] S. E. George *et al.*, "Pulmonary clearance and inflammatory response in C3H/HeJ mice after intranasal exposure to Pseudomonas spp.," *Appl. Environ. Microbiol.*, vol. 59, no. 11, pp. 3585–3591, 1993.

[4] H. A. Cash, D. E. Woods, B. McCullough, W. G. Johanson Jr., and J. A. Bass, "A rat model of chronic respiratory infection with Pseudomonas aeruginosa," *Am.Rev.Respir Dis.*, vol. 119, no. 0003-0805, pp. 453–459, 1979.

[5] S. S. Pedersen, G. H. Shand, B. L. Hansen, and G. N. Hansen, "Induction of experimental chronic *Pseudomonas aeruginosa* lung infection with *P. aeruginosa* entrapped in alginate microspheres.," *APMIS*, 1990.

[6] A. Bragonzi *et al.*, "Pseudomonas aeruginosa microevolution during cystic fibrosis lung infection establishes clones with adapted virulence," *Am. J. Respir. Crit. Care Med.*, vol. 180, no. 2, pp. 138–145, 2009.

[7] M. Facchini, I. De Fino, C. Riva, and A. Bragonzi, "Long Term Chronic Pseudomonas aeruginosa Airway Infection in Mice," *J. Vis. Exp.*, no. 85, pp. 1–10, 2014.

Conclusion and next steps

CONCLUSION AND NEXT STEPS

Antimicrobial resistance has become a global challenge with very slow progress in the development of novel therapies [1]. Most large drug companies have reduced or abandoned infection research due to scientific challenges, and because it has become impossible for them to recoup the cost of research [2]. Actually the pharmaceutical industry focused their research on looking for new antibiotics or improved delivery systems to achieve the target or the site of infection However these approaches only slow the rate of the emergence of multidrug resistance bacteria [3]. The urgently needed to develop alternative approach to classic antimicrobial therapies is real. Actually disruption of quorum sensing can provide an alternative approach to conventional antibacterial therapy, as it targets bacterial virulence rather than bacterial viability. In this way selective resistance is limited without placing life or death pressure on the target bacterium.

In the past decade, the pqs QS system of P. aeruginosa has attracted increasing interest by academic researchers. Pqs QS system plays a fundamental role in the regulation of many virulence mechanisms that are essential for this P. aeruginosa to overwhelm the host in the acute and chronic infection process [4].

In this study we set-up and validate a tailored screening cascade able to aid the selection and the characterization of potential new chemical templates able to modulate the MvfR QS system in *P. aeruginosa*, thus providing new starting points for wider exploration for future lead optimization effort. We have used a structure-based *in silico* screening approach based on docking studies of M64 molecule with the purpose of identifying suitable hits. Compound 21 was identified as the most promising MvfR QSI. It was able to reduced pyocyanin production, HAQs molecules and the pro-persistent 2-AA molecule in *P. aeruginosa* PA14 reference strain at micromolar concentrations. Some small medicinal chemistry modifications were carried out on compound **21** in order to attempt improvement activity. Compound **C**, which was chemical modified by

changing the indole group to an azaindole group, was the only derivative characterized by a higher *in vitro* activity in comparison with compound **21,** both in terms of pyocyanin and HAQs molecules production. Data from the SPR-based assay confirmed that the medicinal chemistry modifications, generating compound **C**, led to a 2 fold increase in binding affinity to the target. Further studies on compound 21 and compound C should be down in order to lead the compound to close pre-clinical phase. The potency of the compounds may vary in a strain dependent manner, thus from a drug discovery point of view, it is important to include multiple strains to validate NCEs in a screening cascade. Actually, we propose as follow step, to test them against the wider *P. aeruginosa* bacterial population involve in cystic fibrosis infections that we have been characterized in the present study. Furthermore, it has been shown that some MvfR QSI are able to increase the susceptibility of *P. aeruginosa* antibiotics [5]. Hence, combination of compound 21 or compound C with some antibiotic appears quite attractive as line of continuation of the present project.

Chronic lung infection rat model induced by intra-tracheal administration of agar beads containing *P. aeruginosa ACC00901 (*preferable than isogenic PAO1 strain) was set –up and validated with Tobramycin. This model is required for understanding the pathogenesis of lung diseases, such as, cystic fibrosis with infecting bacteria and to evaluate new compounds and/or different therapeutic approaches. Even if the model is ready for testing NCEs against *P. aeruginosa* chronic infections, further read outs such as measurement of the host inflammatory response or virulence factors production during the time course of infection will be interesting as next steps.

In summary, we believe the use of quorum sensing inhibitors is a good approach for the development of next-generation anti-infective/anti- virulence therapeutics. However, big anti-infective discovery and development efforts to translate promising hits and lead compounds into clinic are present nowadays in order to enable refilling the pipeline in due time before available treatment options run out.

REFERENCE

[1] H. D. Marston, D. M. Dixon, J. M. Knisely, T. N. Palmore, and A. S. Fauci, 'Antimicrobial resistance', *JAMA - J. Am. Med. Assoc.*, vol. 316, no. 11, pp. 1193–1204, 2016.

[2] J. G. Bartlett, D. N. Gilbert, and B. Spellberg, 'Seven ways to preserve the Miracle of antibiotics', *Clinical Infectious Diseases*. 2013.

[3] A. J. Huh and Y. J. Kwon, '"Nanoantibiotics": A new paradigm for treating infectious diseases using nanomaterials in the antibiotics resistant era', *J. Control. Release*, vol. 156, no. 2, pp. 128–145, 2011.

[4] S. Wagner *et al.*, 'Novel Strategies for the Treatment of Pseudomonas aeruginosa Infections', *J. Med. Chem.*, vol. 59, no. 13, pp. 5929–5969, 2016.

[5] D. Maura and L. G. Rahme, 'crossm Pharmacological Inhibition of the Formation and Potentiates Antibiotic- Mediated Biofilm Disruption', vol. 61, no. 12, pp. 15–17, 2017.

LIST OF ABBREVIATIONS

2-AA	2'-aminoacetophenone
2-ABA	2'-aminobenzoylacetate
2-ABA-CoA	2'-aminobenzoylacetate
AA	anthranilic acid
AI	autoinducer
ATP	adenosine triphosphate
BB	benzamide-benzimidazole
BEW	base equivalent weight
BHL	N-butanoyl-L-homoserine lactone
BLS	bioluminescence
BW	body weight
CAMHB	Cation Adjusted Muller Hinton Broth
CBD	co-inducer binding domain
CDC	Centers for Disease Control and Prevention
CF	cystic fibrosis
CFU	Colony Forming Units
CLSI	Clinical and Laboratory Standards Institute
CO_2	carbon dioxide
CoA	Coenzima A
CS	clinical score
CV	crystal violet
DHQ	2, 4-dihydroxyquinoline
DMF	dimetilformammide
DMPK	Drug Metabolism and Pharmacokinetics
DMSO	dimethyl sulfoxide
DNA	deoxyribo nucleic acid
DNAse	deoxyribonuclease
DTT	dichlorodiphenyltrichloroethane
EARS-Net	European Antimicrobial Resistance Surveillance Network
ECDC	European Centre for Disease Prevention and Control
EDC/NHS	1-Ethyl-3-(3-dimethylaminopropyl)-carbodiimide /N-hydroxysuccinimide
EDR	extreme-drug resistant
EDTA	ethylenediaminetetraacetic acid
EHT	Extended Hückel Theory
EtOAc	Ethyl acetate
FACS	Fluorescence Activate Cell Sorting

FBS	fetal bovine serum
FEV1	forced expiratory volume in the 1st second
Gln	glutamine
HAQs	4-hydroxy-2-alkylquinolines
HHQ	2-heptyl-4-hydroxyquinoline
HIF-1	hypoxia-inducible factor 1
HQNO	N-oxo-2-heptyl-4-Hydroxyquinoline
HTH	helix-turn-helix
HTS	high throughtput screening
IC_{50}	half maximal inhibitory concentration
Ile	isoleucine
IPTG	isopropyl β-D-1-thiogalactopyranoside
iqs	integrating quorum sensing signal
KD	equilibrium dissociation constant
LB	Luria-Bertani
LC/MS-MS	Liquid Chromatography/ Mass Spectometry
LHS	left hand side
LMMD	Low Mode Molecular Dynamics
LogP	partition coefficient
LTTR	LysR-type transcriptional regulators
MBP	Maltose Binding Protein
MDR	multi-drug resistant
MeOH	methanol
MIC	minimal inhibitory concentrations
MMFF	Merck Molecular force field
MOE	Molecular Operating Environment
MTP	microtiter plate
MvfR	multiple virulence factor regulator
MW	molecular weight
na	not available
Na_2SO_4	sodium sulfate
NaCl	sodium chloride
NCE	new chemical entity
NH_4Cl	ammonium chloride
NHQ	2-nonyl-4-hydroxy-quinoline
Ni-NTA	nickel nitrilotriacetic acid
NMR	nuclear magnetic resonance spectroscopy,
NT	not treated

OdDHL	N-(3-oxododecanoyl)-L-homoserine lactone
ODU	optical density units
PBS	phosphate-buffered saline
PDB	Protein Data Base
pMalC2X	plasmid
PQS	*Pseudomonas* quinolone signal
Py-BOP	benzotriazol-1-yl-oxytripyrrolidinophosphonium hexafluorophosphate
QS	quorum ensing
QZN	quinazolinone
RHS	right hand side
rpm	revolutions per minute
RT	room temperature
RU	response unit
SAR	structure-activity relationship
SD	standard deviation
sec	seconds
SPR	surface plasmon resonance
SR	survival rate
TBAF	tetra-n-butylammonium fluoride
TEA	triethylamine
TEV	Tobacco Etch Virus
THF	tetrahydrofuran
Tris-HCl	Tris Hydrochloride
TSB	Tryptic Soy Broth (TSB)
Tyr	tyrosine
v/v	volume/volume
W/V	weight/volume
WHO	World Health Organization

ACKNOWLEDGEMENTS

En primer lugar a Antonio Felici, quien desde el principio ha tenido una gran paciencia conmigo (y hasta el final…). A mis padres, Rosa y Jose, a mi abuela Cari, a mis hermanas Juli y Ana y a mi Carlitos, que han sabido apoyarme desde la distancia durante estos tres años.

No puedo olvidarme de todos mis compañeros de Aptuit, con quienes he trabajado codo con codo, quienes me han ayudado a terminar esta tesis, y de los que he aprendido muchísimas cosas. Mención especial tiene "*la mia mamma italiana*" Isabelle, ya sea en francés, inglés, español o italiano, siempre nos hemos entendido. A Michelito, que habría hecho yo sin su ayuda y su paciencia (que tiene mucha), y como no a Marinella, mi primera guía en esta etapa, y de la que he aprendido muchísimas cosas (sobre todo a no tirar nada, *"nunca se sabe*"). A Daniela, por ensenar a reirme de los problemas, a Vivian por contagiarme (a veces) ese espíritu de investigación que habitualmente brillaba por su ausencia y por ultimo pero no por ello menos importante a Livia, gracias por ensenarme "*a tratar con animales*". A mis amigos, en especial a Francesca, quien me ha abierto los brazos desde el primer día, sin olvidarme de Güidito y Bruno, mis químicos preferidos y mis buenos compañeros del café.

A mis compañeros de Parma y a mi tutor, Andrea Mozzarelli, los cuales indirectamente han tenido también paciencia y me han sabido ayudar en los momentos más críticos. Especialmente a Nina, mi compañera y amiga que durante estos tres años me ha enseñado lo que significa el trabajo duro y constante, "*el que la sigue la consigue*"

Agradecer también a INTEGRATE H2020-MSCA-ITN-2014 y a la Comunidad Europea, quienes me han brindado esta gran oportunidad al inicio de mi carrera.